Pivotal role of Disrupted-in-Schizophrenia 1 (DISC1) in cardiac resilience to ischemic stress

Gurdeep Marwarha[1], Maria J. Pinho[1], Nathan R Scrimgeour[1], Katrine Hordnes Slagsvold[1,2], Alexander Wahba[1,2], Ragnhild E Røsbjørgen[1, 2], Francisco J. Enguita[3], Kun Yang[4], Koko Ishizuka[4], Carlos Andrés Acosta Casas[4], Rajeevkumar Raveendran Nair[5], Rita Brekke[1], Kristine Pettersen[6,7], Geir Bjørkøy[6,7], Akira Sawa[4,8], Morten A Høydal[1]*

[1] Norwegian University of Science and Technology (NTNU), Faculty of Medicine and Health, Department of Circulation and Medical Imaging, Trondheim, Norway.

[2] Dept. of Cardiothoracic Surgery; St. Olavs University Hospital, Trondheim, Norway.

[3] Instituto de Medicina Molecular, Faculty of Medicine, University of Lisbon, 1649-028 Lisbon, Portugal.

[4] Johns Hopkins University School of Medicine, Baltimore, MD.

[5] Norwegian University of Science and Technology (NTNU), Faculty of Medicine and Health, Kavli Institute for Systems Neuroscience (KISN), Trondheim, Norway.

[6] Norwegian University of Science and Technology (NTNU). Department of Biomedical Laboratory Science, Faculty of Natural Sciences, NTNU, Trondheim, Norway.

[7] Norwegian University of Science and Technology (NTNU), Faculty of Medicine and Health, Centre of Molecular Inflammation Research, Department of Clinical and Molecular Medicine, Trondheim, Norway.

[8]Johns Hopkins University School of Public Health, Baltimore, MD.

* Correspondence and requests for materials should be addressed to:

Dr. Morten Andre Høydal

Professor of Medicine

Norwegian University of Science and Technology (NTNU), Faculty of Medicine and Health,Department of Circulation and Medical Imaging,PO Box 8905, NO-7491 Trondheim, Norway.e-mail: morten.hoydal@ntnu.no/ telephone: +4748134843

Summary

Through an unbiased screening at the whole genome level, we underscore that DISC1 is a key molecule for cardiomyocyte resilience post-myocardial infarction. DISC1 has been studied almost exclusively in neuroscience, involving in multiple cellular mechanisms. In contrast, we highlight DISC1's interaction with GSK3β as specific mechanism that drives cardioprotection. We also report DISC1's implication in cardiac health following coronary artery bypass grafting.

Abstract

Molecular targets that contribute to post-myocardial infarction heart failure remains elusive. Here we studied the global transcriptional landscape of human inducible pluripotent stem cell-derived cardiomyocytes under simulated ischemia at the whole genome level in an unbiased manner. Unexpectedly, we identified Disrupted in Schizophrenia 1 (DISC1), which has been almost exlusively studied in neurodevelopment/neurosignaling, as a key molecule. Reduced DISC1 levels increase infarct size in mouse hearts, increases cTnT release following surgery in coronary artery bypass grafting patients and decrease the survival of human AC16 cardiomyocytes exposed to ischemic conditions by disrupting cardioprotective pathways. Mechanistically, the loss of DISC1 interaction with Glycogen Synthase Kinase 3 Beta (GSK3β) heightens GSK3β activity, promoting cell death. Conversely, increasing DISC1 levels enhances cardioprotective signaling by maintaining the DISC1-GSK3β interaction. Although DISC1 is known to interact with many proteins as an intracellular hub, we have identified that its specific interaction with GSK3β is crucial for cardioprotection. These data also indicate that a key molecule involved in brain health and disease also contributes to cardiac health and disease, supporting the idea that neuropsychiatric conditions are systemic.

51 # Introduction

52 Ischemic heart disease, the leading cause of death worldwide,[1] occurs when reduced blood flow causes
53 oxygen deprivation in the heart muscle. This oxygen deprivation, or ischemia, can lead to myocardial
54 infarction, commonly known as a heart attack.[2] Following a myocardial infarction, the activation of
55 various intracellular signaling pathways triggers pathological heart remodeling, further driving disease
56 progression.[3] Numerous efforts have been made to understand these pathological processes, in the
57 hope that better understanding may protect the heart against ischemia, but there is still a major
58 knowledge gap.[2,4-6]
59 To address this challenge, we initially looked at the global transcriptional landscape through next-
60 generation RNA sequencing in human inducible pluripotent stem cell-derived cardiomyocytes (hiPS-
61 cardiomyocytes) subjected to hypoxic stress. Exploring this landscape allowed an identification of novel
62 key transcripts involved in the cardiomyocyte response to hypoxia. Unexpectedly, through an unbiased
63 bioinformatics analysis, disrupted in schizophrenia 1 (DISC1) emerged as the transcript in
64 cardiomyocytes subjected to hypoxic conditions that exhibited the most substantial changes. This robust
65 alteration underscores the potential significance of DISC1 in the cellular response to hypoxia.
66 DISC1 has been studied as an intracellular scaffold protein that plays a key role in neurodevelopment[7,8]
67 In a large Scottish pedigree, the disruption of this molecule is likely to underlie aggregation of psychotic
68 and mood disorders among the family members[9-11]. Accordingly, DISC1 has been studied in the context
69 of neurodevelopment, neurosignaling, and their implications in neurodevelopmental psychiatric
70 disorders[7,12]. To the best of our knowledge, DISC1 has not been studied in cardiology thus far.
71
72 Compared with the general population, patients with psychotic disorders such as schizophrenia are
73 prone to premature death, with a one-to-two-decade reduction in life expectancy[13,14]. Ischemic heart
74 disease is a major reason for this premature mortality[15-17], although antipsychotic medications can also

75 be a contributing factor. Some recent studies have reported deteriorated cardiac function measured by
76 echocardiography and MRI in patients with schizophrenia[18,19]. Myocardial T1 mapping (proton spin-
77 lattice relaxation time), which enables detection of myocardial edema, infarction, ischemia,
78 cardiomyopathies and diffuse fibrosis[20], further suggests that an early diffuse fibroinflammatory
79 myocardial process in patients with schizophrenia is independent of established cardiovascular disease
80 risk factors and could contribute to excess cardiovascular mortality.[19]
81
82 Motivated by the initial global transcriptional mapping that highlighted DISC1, we hypothesized that
83 DISC1 may play a significant role beyond its well-established effects in the brain, specifically addressing
84 its causal mechanism in heart hypoxia. In the present study, we demonstrate that DISC1 plays a crucial
85 regulatory role in heart hypoxia, protecting against cardiac damage caused by ischemic events, such as
86 myocardial infarction. This protective effect is mediated through the regulation of GSK3β activity and its
87 downstream cascade, which ultimately reduces apoptotic cell death.
88

89 # Results

90 ***Global transcriptional profiling and unbiased bioinformatics highlight DISC1 in cardiac hypoxia.***

91 In the initial phase of this project, we employed an unbiased approach to explore unknown signaling
92 cascades in heart hypoxia. We examined the global transcriptional landscape through RNA sequencing
93 (RNA-seq) of human inducible pluripotent stem cell-derived cardiomyocytes (hiPS-cardiomyocytes) that
94 were cultured for 48 hours in a starvation medium and exposed to either 1% O_2 or normoxia as a
95 control. This analysis revealed 1232 significantly regulated coding transcripts (adjusted $P < 0.05$)
96 between hypoxia and normoxia (***Supplements Appendix 1***). To further narrow down the potential novel
97 candidates, we applied stringent statistical criteria with a cut-off $-Log_{10}$ P value $< 10E^{-20}$ and $-Log_2$ fold
98 change (FC) cutoff <-2 or > +2. This approach identified a subset of transcripts that met these criteria:
99 Coiled-Coil Domain Containing 134 (CCDC134), Thyroid Hormone Receptor Alpha (THRA), CKLF Like
100 MARVEL Transmembrane Domain Containing 5 (CMTM5), DISC1, Synaptotagmin 2 (SYT2),
101 Isoprenylcysteine Carboxyl Methyltransferase (ICMT), Zinc Finger Protein 142 (ZNF142), and
102 Thymopoietin (TMPO) (**Fig 1 A-B**).
103
104 To further explore the global transcriptional response to hypoxia in cardiomyocytes, we expanded our
105 bioinformatics analyses by generating regulatory networks using input from the RNA-seq data on both
106 coding and non-coding microRNA transcripts. These analyses focused on negative correlations between
107 overexpressed microRNAs (miRs) and their putative downregulated mRNA targets. Our analyses
108 identified a total of 774 miR-mRNA pairs. DISC1 emerged as the top candidate gene, standing out with
109 the highest number of miR-mRNA interactions, being targeted by 26 specific miRs. Among the other
110 transcripts determined from the statistical cut-off, we found 17 miR-mRNA interactions for CCDC134, 14
111 for ICMT, 8 for TMPO, 4 for SYT2, and none for ZNF142, THRA, and CMTM5. DISC1's prominence

112 underscores its importance among all 1232 significantly regulated coding transcripts (**Fig. 1C** and
113 ***extended data in supplements Appendix 2 and 3***).
114
115 In the RNA sequencing data, DISC1 displayed a downregulation with a Log2FC of -2.67 under hypoxic
116 conditions (P-value = 3.41E-51) (**Fig. 1A-B** and ***supplements Fig. S1, Extended Data in Excel file,***
117 ***Appendix 1***). The robust significant change of DISC1 transcript following hypoxia combined with the
118 number of miRs targeting DISC1, suggests a complex regulatory mechanism, highlighting its potential
119 role in the adaptive response to hypoxic stress. This initial unbiased discovery of DISC1 sparked our
120 interest in understanding its role, which has not been previously described in the context of the heart.
121
122 ***Enrichment of cardiovascular risk gene products among DISC1 interactors***
123 To understand if DISC1 could be an interesting candidate for further analyses we explore the potential
124 involvement of DISC1 in cardiovascular-related conditions from a genetic perspective. From earlier
125 studies in neuroscience, DISC1 is described to acts as a scaffold protein, interacting with numerous
126 proteins to form complex intracellular signaling networks.[7,8] We hypothesized that risk gene products
127 (proteins) associated with cardiovascular conditions may be enriched among DISC1 interactors. To test
128 this, we first identified risk genes for traits linked to cardiologic diseases, malformations, or pathologies
129 (***Supplements Table S1, Data S1***) using data from the NHGRI-EBI GWAS Catalog (criteria: P-value < 1E-8
130 and odds ratio > 1). A chi-square test was then performed to determine whether these risk gene
131 products were overrepresented among DISC1 interactors, compared to non-interacting genes in the
132 human genome.[21] Our analysis revealed a significant enrichment of cardiovascular risk gene products
133 among DISC1 interactors (P-value = 2.8E-17). These findings suggest that downregulation of DISC1 may
134 play a critical role in hypoxia, increasing the heart's vulnerability to ischemic damage.

135

136 Taken together, with a strong support from these unbiased bioinformatic data, we decided to conduct
137 cell biological experiments to validate this notion and address the mechanism of how DISC1 may play
138 this role in the heart and cardiomyocytes.

139

140 ***Biphasic response in DISC1 expression: time and severity-dependent alterations in cardiac ischemia***
141 ***and cardiomyocyte hypoxia***

142 To confirm the presence of DISC1 in cardiomyocytes, as well as the regulation of DISC1 in different
143 models and clinically relevant conditions of ischemic heart disease, we first measured mRNA expression
144 in a rat model of myocardial infarction. Compared to sham-operated rat hearts, DISC1 was significantly
145 upregulated in viable myocardium remote from the infarct area, whereas in the ischemic border zone
146 region, we found unaltered expression of DISC1 transcript (**Fig. 2A**). Analyses in human cardiac left
147 ventricle biopsies from post-myocardial infarction coronary artery bypass grafting (CABG) patients
148 displayed a tendency towards increased DISC1 expression in the remote viable myocardium (**Fig. 2B**),
149 indicating increased DISC1 in response to cardiac ischemia.

150

151 Previous studies from neural cells have reported that the expression of DISC1 is significantly
152 downregulated following hypoxia.[22] These data are in line with our initial discovery of the regulation of
153 DISC1 in cardiomyocytes, where we found that DISC1 was significantly reduced in hiPS-cardiomyocytes
154 stimulated by long-term exposure to hypoxia (48 hours, 1% O_2) (**Fig 1A-B**). Given this contradiction in
155 DISC1 expression compared to less ischemic impacted areas of the heart, we tested shorter timepoints
156 of hypoxia-stimulated cardiomyocytes in culture. Indeed, 6 hours of hypoxia in hiPS-cardiomyocytes
157 significantly increased DISC1 (**Fig. 2C**). The hypoxic response of DISC1 expression was further tested in

158 human AC16 cardiomyocytes, which confirmed a time-dependent response, with DISC1 expression
159 increasing up to 18 hours and thereafter declining to levels below the normoxia baseline at 48 hours and
160 60 hours. (**Fig. 2D-E**). Our data suggest that the initial upregulation of DISC1 expression within the first
161 hours of ischemic/hypoxic stress in cardiomyocytes acts as a compensatory mechanism, potentially
162 conferring protection to the cardiomyocytes and enhancing their resistance to hypoxic conditions.
163 Conversely, the maladaptive response of cardiomyocytes, characterized by reduced or diminished
164 DISC1 expression during prolonged ischemic and/or hypoxic stress, may exacerbates ischemic damage
165 to the heart and cardiomyocytes. Therefore, to further investigate the role of DISC1 in ischemic damage,
166 we examined whether downregulation of DISC1 influences myocardial infarction size.
167
168 ***Downregulation of DISC1 increases myocardial infarction size***
169 To test whether downregulation of DISC1 causes greater ischemic damage, we used a mouse model with
170 a DISC1-locus deletion (DISC1-locus impairment (DISC1-LI), as previously described.[8] We found that
171 downregulation of DISC1 caused significantly larger infarct size following ischemia-reperfusion in a
172 Langendorff coronary perfusion infarct model of thirty minutes of global ischemia followed by 2 hours of
173 reperfusion in isolated DISC1-Li mouse hearts vs. wild type (WT) mouse hearts. DISC1-Li mice displayed
174 larger infarct sizes in both male (130% larger) and female mice (73% larger) (**Fig. 3A-C**). These data
175 strengthen the hypothesis that downregulation of DISC1 indeed exacerbates ischemic damage.
176
177 ***Low expression levels of DISC1 RNA in blood correletes with increased release of cardiac troponin T***
178 ***(cTnT) following CABG surgery***
179 Based on the significantly increased infarct size in mice with downregulated DISC1 we aimed to verify
180 our findings in a clinical study from CABG patients, a setting where all patients underwent peroperative

181 cardiac ischemia-reperfusion due to aortic cross-clamping, as reflected by postoperative release of
182 cTnT.[23-25] Therefore, we investigated whether there was a correlation between low DISC1 RNA
183 expression in blood and increased cTnT release from pre- to 24 hours post-CABG surgery, as a marker of
184 ischemia-reperfusion injury. Our analysis revealed that patients with lowest DISC1 RNA levels displayed
185 highest cTnT release 24 hours post-surgery (Pearson correlation, r = -0.32, P = 0.045, **Fig. 3D**). These
186 findings validate our hypothesis and emphasize the clinical significance of DISC1 in enhancing cardiac
187 resilience to ischemia.
188

189 ***Downregulation of DISC1 exacerbates cardiomyocyte vulnerability to hypoxic stress trough activation***
190 ***of GSK3β while overexpression of DISC1 reverses these effects***

191 Oxygen and nutrient deprivation triggers metabolic acidosis, calcium overload, and reactive oxygen
192 species (ROS), leading to mitochondrial depolarization, swelling, and opening of the mitochondrial
193 permeability transition pore (mPTP),[26,27] ultimately resulting in cell death.[28-30] To gain deeper
194 mechanistic insights into the impact of modified DISC1 expression on cardiomyocyte death, we
195 employed shRNA-DISC1 for silencing and a DISC1 expression vector for overexpression. We found that
196 silencing of DISC1 significantly sensitized cardiomyocytes to 18 hours of hypoxic stress and increased the
197 activity of GSK3β (**Fig. 3E**), which culiminated in increased cell death assayed by lactate dehydrogenase
198 (LDH) release (**Fig. 3F**). Further analyses verified activation of established downstream signalling
199 processes, including BAX's interaction with the outer mitochondrial membrane (OMM), resulting in
200 membrane permeabilization, CytC release, and the activation of caspase-3 (***Supplements Fig. S2-5***).
201 Importantly, overexpression of DISC1 inhibited the activation of GSK3β (**Fig. 3E**) and reversed
202 downstream cell death signaling processes (**Fig. 3F**, ***Supplements Fig. S2-5***). These data confirm an

203 important role of DISC1 in suppressing GSK3β activity, leading to enhanced cardiomyocyte resistance
204 against hypoxia-induced cell death[31].
205

206 ***Causative link between DISC1- GSK3β interaction for the regulation of cell death signaling?***

207 To this point we have comprehensively investigated the role of DISC1; we meticulously examined its
208 impact on GSK3β activation, and confirmed known signalling processes of hypoxia induced cell death
209 which were amplified with silencing of DISC1 and mitigated by overexpression of DISC1. We also
210 confirmed that there exist a direct interaction between DISC1 and GSK3β by Co-IP in human AC16
211 cardiomyocytes (***Supplements Fig S6***). However, a lingering question remained: can the enhanced
212 GSK3β activity observed in cells with downregulated DISC1, and conversely, the reduced GSK3β activity
213 in cells with overexpressed DISC1, be attributed to a direct interaction between DISC1 and GSK3β? To
214 address this question, we designed additional experiments where we assessed the effect of interrupting
215 the binding between DISC1 and GSK3β.
216

217 First, we designed a new overexpression vector with a triple mutant and replaced Phenylalanines (F)
218 with Alanine (A) at the sites (F210, F212 and F206) in the full length DISC1 (3AAA mutant), that would
219 not allow for DISC1- GSK3β interaction, based on a previous report that the residues 193−236 from the
220 full-length protein are the most potent GSK3β binding region of DISC1.[32] To avoid an effect of the DISC1
221 shRNA on the overexpression product, silent nucleotide mutations at the target sequence of the DISC1
222 shRNA were included into the overexpression vector, thus hindering the silencing of the expressed 3AAA
223 mutant or wild type DISC1. Using this approach the expressed product of DISC1 should be a DISC1-3AAA
224 mutant resistant to RNAi (DISC1- $\Delta GSK3\beta^R$) or full length (FL) wild type DISC1 resistant to RNAi (DISC1-
225 FL^R). Then, we verified the DISC1- $\Delta GSK3\beta^R$ effect for DISC1- GSK3β interaction using Co-

226 Immunoprecipitation (Co-IP). We found that the interaction between for DISC1- GSK3β was significantly
227 reduced in the DISC1-ΔGSK3β^R, confirming that mutating the F210, F212 and F206 sites hinder
228 interaction (**Fig. 4A**).
229
230 To further assess the role of DISC1 on GSK3β activity during hypoxia, we repeated the experiments using
231 the DISC1-FL^R and compared this to GSK3β activity using the DISC1-ΔGSK3β^R. We found that the GSK3β
232 activity was increased in presence of DISC1 shRNA with wild type full length DISC1 that is not resistant to
233 shRNA (DISC1 RNAi); GSK3β activity was significantly reduced by overexpression of the DISC1-FL^R vector
234 (DISC1 RNAi + DISC1-FL^R). We also found a modest reduction in GSK3β activity using the DISC1-ΔGSK3β^R
235 vector (DISC1 RNAi + DISC1-ΔGSK3β^R), but most importantly this effect was significantly less than the
236 findings from DISC1-FL^R. Collectively, these data display that a direct interaction between DISC1 and
237 GSK3β is a major component of the mechanism(s) underlying reduced GSK3β activity by overexpression
238 of DISC1 (**Fig. 4B**).
239
240 To further determine the downstream effects of the GSK3β-DISC1 interaction, we used the same
241 experimental design and performed CytC and caspase-3 activity assay. CytC release to cytosol was high
242 when DISC1 was silenced by shRNA DISC1 (DISC1 RNAi), which was rescued by overexpression of DISC1
243 by DISC1-FL^R vector resistant to shRNA (DISC1 RNAi + DISC1-FL^R), but not by DISC1- ΔGSK3β^R (DISC1 RNAi
244 + DISC1-ΔGSK3β^R) (**Fig. 4C**). These data were also confirmed for the Caspase-3 activity (**Fig. 4D**). LDH
245 released from cardiomyocytes to the medium as a marker for cell death confirmed the same results (**Fig.
246 4E**). The collective evidence from these studies unequivocally establishes the crucial role of the direct
247 interaction between DISC1 and GSK3β in conferring protection against cell death induced by hypoxic
248 conditions. This interaction in cell death signaling processes is pivotal in maintaining the resilience of

249 cardiomyocytes under hypoxic stress. The disruption of this interaction significantly compromises the
250 resistance of cardiomyocytes to hypoxia, rendering them highly susceptible to cell death.
251

252 Discussion

253 Cardioprotective therapies targeting reperfusion-related injury remain among the top 10 unmet clinical
254 needs in cardiology.[4-6,33] This study addresses these existing gaps and sheds light on a discovery that may
255 hold significant implications for addressing key components of ischemic damage on the heart. The
256 unbiased identification of DISC1 in an *in vitro* cardiomyocyte model of ischemia, as unveiled by RNA
257 sequencing, sparked scientific interest in the potential role of DISC1 as a novel regulator of signaling
258 pathways integral for ischemic cardioprotection. This discovery was further substantiated by GWAS
259 enrichment analyses demonstrating an overrepresentation of risk gene products for cardiologic diseases
260 among DISC1 protein interactors.
261
262 In this study, we present evidence of a major detrimental effect of reduced DISC1 protein levels on
263 myocardial infarct size in mouse hearts, correlation between low expression levels of DISC1 and
264 increased cTnT release that indicate more severe ischemia- reperfusion injury following surgery in CABG
265 patients, as well as *in vitro* cardiomyocyte survival. Increased ischemic damage is due to the disruption
266 of signaling pathways that are critical for cardioprotection. Although DISC1 is known to interact with
267 many proteins as an intracellular hub, we have pinpointed that its specific interaction with GSK3β is
268 essential for cardioprotection. Specifically, we show that reduced DISC1 levels in cardiomyocytes limits
269 the ability for DISC1 to bind directly to GSK3β and silence the downstream cell death signalling induced
270 by GSK3β activation. In stark contrast, the augmentation of DISC1 protein levels resulted in enhanced
271 cardiomyocyte survival and the activation of cardioprotective signaling via via maintenance of direct
272 DISC1- GSK3β interaction which inhibited the GSK3β activity.

273

274 At the mechanistic level, our data on increased cardiomyocyte injury following ischemic and hypoxic
275 challenges by DISC1 depletion are explained by activation of apoptotic signaling trough GSK3β
276 activation. Here, we reported that knockdown of DISC1 enhanced the activation of GSK3β, whereas
277 overexpression of DISC1 reduced GSK3β activity through direct interaction. These data are important, as
278 recent studies have demonstrated that GSK3β inhibition contributes to cardiac protection in both
279 preconditioning [34] and postconditioning.[35,36] This protection due to GSK3β inhibition has been linked to
280 hindering opening of the mPTP [34,36-38] and reduced BAX integration in the mitochondrial membrane and
281 MAC pores formation,[39,40] consequently reducing the release of proapoptotic molecules such as CytC
282 and activation of caspase-3, which is the key regulatory event that induces terminal effector events in
283 the apoptotic cascade.[41-44 45] All these effects were verified in the present study. Our investigation
284 illuminates the pivotal role of DISC1 as a central conductor within the myocardium, coordinating a
285 network of intracellular processes that collectively confer protection against ischemic heart disease. The
286 importance of maintaining elevated levels of DISC1 for cardioprotection against ischemia-induced cell
287 death is underscored, particularly in light of its direct interaction with GSK3β.

288

289 The biphasic expression of DISC1 following ischemic/hypoxic stress is noteworthy. Our data indicate that
290 during the initial phase, DISC1 expression is elevated, suggesting the activation of protective
291 compensatory mechanisms. However, under conditions of chronic, persistent cellular hypoxia, DISC1
292 expression diminishes. Maintaining DISC1 levels, *i.e.*, the ability to resist this reduction during
293 ischemia/cellular hypoxia, appears crucial for survival. At the molecular level, DISC1 functions as a
294 shield, mitigating the harmful effects of hypoxia on cardiomyocytes. When this shield is compromised or
295 lost, cardiomyocytes become vulnerable, resulting in an increased rate of cell death. This vulnerability
296 leads to a higher incidence of cell death and more extensive myocardial infarction following cardiac

297 ischemia which also were displayed trough the correlation between low DISC1 RNA expression in blood
298 and increased release of cTnT following surgery in CABG patients.
299
300 Given that DISC1 protein stability may be enhanced by Phosphodiesterase 4B (PDE4B)[22], and considering
301 that PDE4 is a prominent target in drug discovery and development, medications targeting PDE4 could
302 potentially be applied or repurposed in this context. The mechanism of DISC1 downregulation remains
303 unclear, and to date, there have been no significant efforts to elucidate the transcriptional mechanisms
304 regulating DISC1. Investigating the transactivation and stability of DISC1 mRNA could represent a novel
305 approach for drug discovery. Additionally, the role of the 26 specific overexpressed miRs in regulating
306 DISC1 protein stability warrants further exploration. These miRs have been identified as key regulators
307 that may influence DISC1 levels by targeting its mRNA, thereby affecting its stability and expression. The
308 role of miRs as regulatory factors of the DISC1 interactome has also been previously addressed in
309 neuronal cells.[21] Studying these miRs could provide valuable insights into maintaining DISC1 levels and
310 developing novel therapeutic strategies for cardioprotection. Consequently, understanding the
311 transcriptional and post-transcriptional regulation of DISC1 is crucial for developing interventions aimed
312 at preserving its protective functions in both neuronal and cardiac contexts.
313

314 # Materials and methods

315 ***RNA sequencing data - Library construction and sequencing***

316 RNeasy Mini Kit from Qiagen (Qiagen Norge, Oslo, Norway) was used for RNA extraction according to
317 the manufacturer's instructions. RNA concentration was measured using a Qubit® RNA HS Assay Kit on a
318 Qubit® 3.0 Fluorometer (Thermo Fisher Scientific Inc., Waltham, MA, USA). Integrity was assessed using
319 an Agilent RNA 6000 Pico Kit on a 2100 Bioanalyzer instrument (Agilent Technologies, Santa Clara, CA,
320 USA).
321 RNA sequencing libraries were prepared using a TruSeq Stranded mRNA kit (Illumina, San Diego, CA,
322 USA) according to the manufacturer's instructions. In brief, 300 ng of total RNA was used as the starting
323 material. First, mRNA was purified from the total RNA using poly-T oligo-attached magnetic beads,
324 followed by random fragmentation using divalent cations at 94°C for 4 min. First- and second strand
325 cDNAs were synthesized using random oligonucleotides and SuperScript II, followed by DNA polymerase
326 I and RNase H. Exonuclease/polymerase was used to produce blunted overhangs. Illumina dual index
327 adapter oligonucleotides were ligated to cDNA after 3' end adenylation. DNA fragments were enriched
328 by 15 cycles of PCR. The libraries were purified using AMPure XP (Beckman Coulter, Inc., Indianapolis, IN,
329 USA), quantitated by qPCR using the KAPA Library Quantification Kit (Kapa Biosystems, Inc., Wilmington,
330 MA, USA) and validated using the Agilent High Sensitivity DNA Kit on a Bioanalyzer (Agilent
331 Technologies, Santa Clara, CA, USA). The size range of the DNA fragments was measured to be in the
332 range of app. 200-1000 bp and peaked around 285 bp.
333 Libraries were normalized and pooled to 2.7 pM and subjected to clustering on two NextSeq 500 high
334 output flow cells (Illumina, San Diego, CA, USA). Finally, single-read sequencing was performed for 75
335 cycles on a NextSeq 500 instrument (Illumina, Inc. San Diego, CA, USA) according to the manufacturer's
336 instructions. Base calling was performed on a NextSeq 500 instrument by RTA 2.4.6. FASTQ files were

337 generated using bcl2fastq2 Conversion Software v2.20.0.422 (Illumina, Inc. San Diego, CA, USA). FASTQ
338 files were filtered and trimmed (fastp v0.20.0), and transcript counts were generated using quasi
339 alignment (Salmon v1.3.0) to the transcriptome reference sequence (Ensembl, GRCh38 release 103).
340 Transcript sequences were imported into R statistical software and aggregated to gene counts using the
341 tximport (v1.14.0) bioconductor package. Gene counts were normalized and analyzed for differential
342 expression using the DESeq2 bioconductor package. DESeq2 is a specialized software for the analysis of
343 RNA-seq data that builds a generalized linear model under the assumption of negative binomial
344 distributed values and uses the Wald statistic for significance testing.
345

346 ***Regulatory networks in hypoxia-stimulated hiPSC-CM relationships between upregulated miRs and***
347 ***their downregulated mRNA targets***

348 Establishing functional relationships between those differentially expressed RNAs, we generated
349 regulatory networks that depicted negative correlations between overexpressed miRNAs and their
350 putative downregulated mRNA transcripts. Regulatory networks in hypoxia-stimulated hiPSC-CM were
351 displayed by the predicted functional relationships between upregulated miRs and their downregulated
352 mRNA targets. All predictions were made by using the MiRWalk 2.0 algorithm.[46] Protein-protein
353 interactions were extracted from the STRING database.[47] ***Supporting material for analyses included in***
354 ***separate Excel file, Appendix 3.***
355

356 ***Cardiac patient biopsies and blood samples***

357 Biopsies were obtained from patients scheduled for elective CABG surgery at St. Olavs Hospital,
358 Trondheim, Norway (stored in local biobank: ID275364). The patients were post-MI <15 days prior to

359 CABG surgery (MI, N=5) versus patients with no previously defined MI (control, N=4). Biopsies were
360 taken before aortic cross-clamping from nonfibrotic and viable left ventricle mid-myocardium in the
361 remote noninfarcted area using a BioPince™ needle from Angiotech Pharmaceuticals, Inc. (Vancouver,
362 Canada) and snap-frozen in liquid nitrogen. All perioperative procedures were performed according to
363 standard routines of the department. Approved by the Regional Committee for Medical and Health
364 Research Ethics (REK), Norway (Study Id numbers 285936).
365
366 Blood samples were taken from locally stored and approved (REK ID 275364) biobanked samples from
367 patients undergoing CABG surgery at St. Olavs Hopsital, Trondheim Norway (N=29) (patients
368 characteristics are presented in ***Supplements Table S2***. The specific project testing the hypothesis that
369 low DISC1 RNA expression in blood causes more cardiac ischemia-reperfusion injury during CABG
370 surgery, measured by increased cardiac Troponin T (cTnT) levels, was approved by REK, Norway (Study
371 Id numbers 560077). High sensitive cTnT was analysed from blood serum samples by immunoassay
372 (Elecsys Troponin T hs, Instrument Roche cobas 8000) at the at the Department of Medical Biochemistry
373 at St. Olavs Hospital, Trondheim, Norway that is accredited according to the NS-EN ISO 15189 laboratory
374 standard. DISC1 RNA in blood was analysed from whole blood samples stored at 80ºC freezer in
375 PAXgene Blood RNA Tube (PreAnalytiX,Qiagen, Hilden, Germany).
376 Blood samples of DISC1 RNA was analysed from the timepoint pre surgery. cTnT blood samples was
377 analysed as delta difference from pre surgery to 24 hours post surgery.
378

379 ***Animal studies***

380 The mouse model was a DISC1 locus impairment (DISC1-Li) mouse model that is based on a C57BL/6
381 background with a locus deletion that included the *Tsnax*/*Trax* gene located at 5' to the *Disc1* gene was

382 included to the study. The 40-kb locus deleted covers exons 1, 1b, 2 and 3 and depletes *Tsnax*/*Trax-*
383 *Disc1* intergenic splicing. miRNA in intron 1, which could alter the functions and levels of DISC1 by
384 targeting at least some DISC1-binding partner genes (such as 14-3-3 and CRMP1/2), was also deleted, as
385 previously described.[8] (Approved by the Norwegian Animal Research Authority (NARA), Id:13651).
386 Experiments using post myocardial infarction in rats were performed by permanent occlusion of the left
387 anterior descending (LAD) coronary artery, as previously described.[48] Sham surgery was performed
388 without ligation. Following MI, the animals remained in their cages before they were killed after 4
389 weeks. (NARA, Id: 9768).
390
391

392 ***Langendorff perfused hearts***

393 Global ischemia was performed *ex vivo* on isolated mouse hearts using Langendorff perfusion. The
394 laboratory perfusionist was blinded to the animals included. All animals experiments were performed in
395 randomized order. After removal of the heart, the aorta was cannulated, and the heart was perfused
396 with Krebs-Hensleit solution with a stable aortic pressure of 60 mmHg and immersed in a bath. Solutions
397 were bubbled with 95% O_2/5% CO_2 and maintained at 37°C. After 20 mins of perfusion, the hearts were
398 subjected to 30 mins of ischemia by stopping the perfusion flow. Hearts were then reperfused for 1 h 40
399 m before being taken down and frozen at -20°C overnight. The following day, hearts were cut into 1.5
400 mm transverse sections using a heart slicing matrix and incubated for 10 minutes in 1% 2,3,5-
401 triphenyltetrazolium chloride (TTC) shaking at 37°C. Slices were placed in PBS between glass slides and
402 scanned at 3200 dpi using a flatbed scanner. The second and third slices closest to the apex were used
403 for analysis. Intensity thresholds were determined by a blinded third party to discriminate between
404 black (background), red (viable tissue) and white (nonviable tissue). The percentage of nonviable tissue

405 in a heart was measured by calculating the percentage of white pixels as a total of all non-background
406 pixels across the two section scans. All image analyses were performed using ImageJ. (NARA id: 13651).
407 Exlusion criterias to the study was unsuccesfull Langendorff perfusion and hearts that where not able to
408 mount on the perfusion system.
409

410 ***Cell culture and treatments***

411 Human AC-16 cardiomyocyte cells (EMD Millipore / Merck Millipore / Merck Life Sciences, Catalogue #
412 SCC109, Darmstadt, Germany, RRID:CVCL_4U18) were cultured in Dulbecco's modified Eagle's medium
413 (DMEM): Ham's F12 (1:1; v/v) with 2 mM Glutamine, 12.5% fetal bovine serum (FBS), and 1%
414 antibiotic/antimycotic mix, Following the established guidelines, procedures, and protocols set by the
415 commercial vendor. To conduct gain-of-function and loss-of-function experiments, AC-16 cells were
416 subjected to reverse transfection in suspension using the DISC1 overexpression vector (Full length DISC1
417 isoform L ((https://www.uniprot.org/uniprotkb/Q9NRI5/entry#Q9NRI5-1; Transcript: Human
418 NM_018662.3) pRK5-DISC1 overexpression) or the vector encoding *DISC1* shRNA (TRC Lentiviral Human
419 DISC1 shRNA, Dharmacon / Horizon Scientific, Cambridge, UK, Catalogue # RHS3979-201826869, Clone
420 Id: TRCN0000118997; mature antisense sequence TTAATGATCTAATCTCCTCGG).
421

422 For experiments to determine the direct association of DISC1-GSK3 interaction we used the pRK5 vector
423 systems with the following modification: Based on domain of DISC1 that is crucial for binding to
424 GSK3(193−236) from the full-length protein sequence and the most potent GSK3β binding region of
425 DISC1[32] we created a triple mutant where Phenylalanines (F) was replaced by Alanine (A) at the sites.
426 Using the pRK5 myc-hDISC1 plasmid as a template, we introduced the F206A, F210A, and F212A
427 mutations into the hDISC1 sequence. Subsequently, we generated an escape mutant resistant to shRNA

428 (^{R}) on the pRK5 myc-hDISC1 full length (DISC1-FL) and the pRK5 myc-hDISC1 F206A, F210A, F212A
429 constructs by mutating the binding site sequence of the DISC1 shRNA while preserving the original
430 amino acid sequence of hDISC1 (Name used in the paper for constructs: **DISC1- ΔGSK3β^R** and **DISC1-FL^R**.
431 This approach would avoid an effect of GSK3β interacting with the endogenous DISC1 and at the same
432 time is not able to silence either the the overexpressed **DISC1-FL^R** or the **DISC1- ΔGSK3β^R**.
433 The escape mutant was designed based on the same vector encoding *DISC1* shRNA; antisense sequence
434 TTAATGATCTAATCTCCTCGG obtained from, RHS3979-201826869, Clone Id: TRCN0000118997. The
435 complete sequences of the relevant constructs produced in this paper are provided in ***supporting data***
436 ***Appendix 4.***
437
438 To overexpress or knock-down *DISC1* expression, AC-16 cells were transfected in suspension *(reverse*
439 *transfection*) with the respective vectors, using Polyfect® (Qiagen Norge, Oslo, Norway, Catalogue #
440 301107) in accordance to the manufacturer's guidelines and standardized procedures [49,50]. The plasmid
441 load to be transfected was standardized to 1 µg per 0.6 x 10^6 cells and *scaled-up* or *scaled-down* in
442 accordance to the stipulations of the experimental paradigm [49,50]. The hypoxia challenge (1% O_2, 5% CO_2,
443 and 94% N_2) was effectuated by incubating the transfected AC-16 cells with the specific *hypoxia medium*
444 (***Supplementary Table S3***). The hypoxia challenge was induced and maintained for the designated
445 duration using the *New Brunswick™ Galaxy® 48 R CO_2 incubator* (Eppendorf Norge AS, Oslo, Norway).
446 For RNA sequencing of hIPS-CMs vials of 1 × 10^6 Cor.4U cardiomyocytes were seeded in gelatin pre-
447 coated 48-well plates and maintained in Cor.4U Complete Culture Medium total RNA was extracted
448 from hIPS-cardiomyocytes (Cor.4U cardiomyocytes (Ncardia, Cologne, Germany), that was treated by
449 either by 48 hours in hypoxia or normoxic control conditions at the temperature of at 37°C using the
450 same procedure as for AC16 cardiomyocytes. Cells were thereafter harvested and immediately snap
451 frozen and stored at -80°C freezer for subsequent RNA extraction.

452

453

454 ***DISC1 ELISA***

455 The DISC1 protein levels in experimental lysates were measured by using a *sandwich* ELISA
456 immunoassay approach. Briefly, 10 ng of DISC1 *capture* antibody (***Supplementary Table S4***) was
457 immobilized in each well of a 96-well microplate. The experimental cell lysates (equivalent to 50 µg of
458 protein content) were incubated with the immobilized DISC1 *capture* antibody, overnight at 4^0C. The
459 conditioned cell lysate was discarded, the 96-well microplate wells were washed 3x (15 minutes each)
460 with TBS-T (Tris-buffered saline with 0.1% v/v Tween-20) and incubated with the DISC1 *detection*
461 antibody (***Supplementary Table S4***), overnight at 4^0C. The 96-well microplate wells were washed 3x (15
462 minutes each) with TBS-T followed by immunodetection with the HRP (horseradish peroxidase)-
463 conjugated secondary antibody using the HRP-substrate TMB (3,3',5,5'-Tetramethylbenzidine) (Thermo
464 Fisher Scientific, Oslo, Norway, Catalogue # N301) as a chromophore for the colorimetric read-out (λ_{450}).
465 The antibody and signal specificity were established by performing *peptide blocking assay* in the entire
466 gamut of experimental lysates. The DISC1 antibody blocking peptide corresponding to the specific
467 epitope for the DISC1 *detection* antibody (***Supplementary Table S4***) was used for the *peptide blocking*
468 *assay*. The respective optical density (O.D) values from the *peptide blocking assay* were used for
469 experimental blank correction. Data is expressed as experimental blank corrected $O.D_{450}$ (λ_{450}) values
470 from three technical replicates for each of the four biological replicates belonging to each experimental
471 group (n = 4).

472

473 ***Lactate Dehydrogenase (LDH) Assay***

474 Lactate Dehydrogenase (LDH) levels in the conditioned media were assessed as an indicator of general
475 cell death. The measurement of LDH levels in the conditioned medium was performed using a sandwich
476 ELISA immunoassay technique as previously described.[40] 20 ng of LDH capture antibody (see
477 ***Supplementary Table S4***) was attached to each well of a 96-well microplate. Experimental sample
478 conditioned media (50 µL) were then incubated with the immobilized LDH capture antibody overnight at
479 4°C. The conditioned media was removed, and the wells of the 96-well microplate were washed three
480 times (15 minutes each) with TBS-T (Tris-buffered saline with 0.1% v/v Tween-20). The wells were then
481 incubated overnight at 4°C with LDH-A and LDH-B detection antibodies (***Supplementary Table S4***). After
482 incubation, the wells were washed again three times (15 minutes each) with TBS-T, followed by
483 immunodetection using an HRP-conjugated secondary antibody. The HRP-substrate OPD (o-
484 phenylenediamine dihydrochloride) (Thermo Fisher Scientific, Oslo, Norway, Catalogue # 34005) was
485 used as a chromophore for the colorimetric read-out at 450 nm (λ450). Antibody and signal specificity
486 were confirmed through peptide blocking assays across all experimental lysates. The LDH-A and LDH-B
487 antibody blocking peptides (***Supplementary Table S4***) were used for these assays. Optical density (O.D)
488 values from the peptide blocking assays were utilized for experimental blank correction. Data is
489 presented as experimental blank corrected O.D450 (λ450) values from three technical replicates for
490 each of the four biological replicates in each experimental group (n = 4).
491

492 ***Cellular fractionation to segregate the cytosolic and mitochondrial compartments***

493 Cellular fractionation to obtain the cytosolic and mitochondrial fractions was carried out using the
494 "Mitochondria/Cytosol Fractionation Kit" from Abcam (Catalogue # ab65320, Abcam, Cambridge, UK),
495 following the manufacturer's instructions as previously described.[40] AC-16 cells were terminally sub-

496 cultured and plated in 150 mm cell-culture plates to reach the desired confluence (2 x 10^7 cells per
497 plate). After undergoing the specified transfection and experimental procedures, the cells were
498 trypsinized and pelleted by centrifugation at 1000 x g for 5 minutes at 4°C. The cell pellets were then
499 resuspended in 1x Cytosol Extraction Buffer Mix containing DTT (dithiothreitol) and protease inhibitors
500 (provided with the kit) and incubated on ice for 10 minutes. The cells were homogenized on ice using a
501 Dounce homogenizer with 30-50 strokes. The resulting cell lysate was transferred to a 1.5-mL
502 microcentrifuge tube and centrifuged at 700 x g for 10 minutes at 4°C. The supernatant was collected
503 (discarding the pellet) and further centrifuged at 10000 x g for 30 minutes at 4°C. The supernatant
504 obtained constituted the cytosolic fraction, while the pellet represented the mitochondrial fraction. The
505 mitochondrial pellet was either resuspended in 100 µL of 1x PBS (pH 7.4) to obtain intact mitochondria
506 or in 100 µL of Mitochondrial Extraction Buffer Mix (with DTT and protease inhibitors) to obtain the total
507 mitochondrial fraction. Both the cytosolic and mitochondrial fractions were then processed for sandwich
508 ELISA immunoassays to verify their integrity. The mitochondrial fraction's integrity was confirmed by the
509 presence of COX4 (Cytochrome C Oxidase Subunit 4) and the absence of β-Actin, while the cytosolic
510 fraction's integrity was validated by the absence of COX4 and the presence of β-Actin.
511

512 ***Cytochrome C Release Assay***

513 The movement of Cytochrome C from the inter-mitochondrial space to the cytosol was assessed by
514 comparing its relative abundance in the cellular and mitochondrial fractions. The levels of Cytochrome C
515 in these fractions were quantified using a sandwich ELISA immunoassay method as previously outlined.[40]
516 Briefly, 20 ng of the Cytochrome C *capture* antibody (***Supplementary Table S4***) was immobilized in each
517 well of a 96-well microplate. The respective cytosolic fractions (equivalent to 50 µg of protein content)
518 and mitochondrial fractions (equivalent to 20 µg of protein content) were incubated with the

519 immobilized Cytochrome C *capture* antibody, overnight at 4^0C. The conditioned cytosolic fractions and
520 mitochondrial fractions were discarded and the 96-well microplate wells were washed 3x (15 minutes
521 each) with TBS-T and incubated with the Cytochrome C *detection* antibody (***Supplementary Table S4***),
522 overnight at 4^0C. The 96-well microplate wells were washed 3x (15 minutes each) with TBS-T followed by
523 immunodetection with the HRP-conjugated secondary antibody, using the HRP-substrate OPD, as a
524 chromophore for the colorimetric read-out (λ_{450}). The antibody and signal specificity were established by
525 performing *peptide blocking assay* in the entire gamut of experimental lysates. The Cytochrome C
526 antibody blocking peptide (Cell Signaling Technology, Danvers, MA, USA, Catalogue # 1033)
527 corresponding to the specific epitope for the Cytochrome C antibody (***Supplementary Table S4***) was
528 used for the *peptide blocking assay*. The respective absorbances from the *peptide blocking assay* were
529 used for experimental blank correction. Data is expressed as experimental blank corrected $O.D_{450}$ (λ_{450})
530 values from three technical replicates for each of the four biological replicates belonging to each
531 experimental group (n = 4).
532

533 ***Caspase-3 Activity Assay***

534 The enzymatic activity of caspase-3 was assessed spectrophotometrically using the specific substrate Ac-
535 DEVD-p-NA (N-Acetyl-Asp-Glu-Val-Asp-p-nitroanilide) (Sigma Aldrich, Oslo, Norway, Catalogue # 235400-
536 5MG) as previusoly described.[40] Caspase-3 activity was inferred from the amount of chromophore
537 released due to the proteolysis of Ac-DEVD-p-NA by caspase-3. Briefly, AC-16 cells were terminally sub-
538 cultured and plated in 100 mm cell-culture plates to reach the desired confluence (4 x 10^6 cells per
539 plate). After undergoing the specified transfection and experimental procedures, the cells were
540 trypsinized and pelleted by centrifugation at 1000 x g for 5 minutes. The cell pellets were resuspended
541 in cell lysis buffer (50 mM HEPES, 5 mM CHAPS, pH 7.4) and incubated on ice for 10 minutes to lyse the

542 cells, followed by centrifugation at 12000 x g for 15 minutes to pellet the cell debris. The supernatant
543 containing non-denatured cell lysates (without protease inhibitors) was used for caspase-3 activity
544 determination. The protein concentration of the non-denatured cell lysates was adjusted to 4 µg/µL,
545 and the volume was brought to 180 µL with assay buffer (20 mM HEPES, 1.62 mM CHAPS, 10 mM NaCl,
546 2 mM EDTA, pH 7.4). For the caspase-3 activity assay, 200 µg of protein (50 µL of lysate at 4 µg/µL
547 diluted to 180 µL) per well of a 96-well microplate was used from each experimental sample. The
548 samples were incubated with the caspase-3 substrate, Ac-DEVD-p-NA (200 µM, 20 µL of 2 mM in a 200
549 µL assay volume), for 4 hours at 37°C. Caspase-3 activity assays were also conducted in the presence of
550 the caspase-3 inhibitor, Ac-DEVD-CHO (Sigma Aldrich / Merck Millipore / Merck Life Science, Darmstadt,
551 Germany, Catalogue # 235420), to confirm assay specificity and serve as an experimental blank.
552 Absorbance at 405 nm (λ405), corresponding to the amount of chromophore produced as a measure of
553 caspase-3 activity, was determined using a microplate reader. Absorbance values from caspase-3
554 inhibitor-treated lysates were used for experimental blank correction. Data is presented as experimental
555 blank corrected O.D405 (λ405) values from three technical replicates for each of the four biological
556 replicates in each experimental group (n = 4).
557

558 ***GSK3β kinase activity assay***

559 GSK3β kinase activity in non-denatured experimental lysates was assessed using an Indirect ELISA
560 immunoassay. The phosphorylation level of the serine residue in the synthetic peptide
561 (RRRPASVPPSPSLSRHS(pS)HQRR), which corresponds to the GSK3β consensus recognition motif in the
562 endogenous substrate muscle glycogen synthase 1 ((pS) indicates phosphorylated-serine), served as a
563 surrogate marker for GSK3β kinase activity in the experimental lysates. 96-well microplates were
564 prepared using Streptavidin-Biotin chemistry. Initially, the wells were coated with 20 pmoles (1.1 µg) of

565 Streptavidin (110 µL of 10 µg/mL Streptavidin in 20 mM potassium phosphate, pH 6.5). This was
566 followed by the immobilization of the biotinylated-GSK3β substrate (GSM [GSK3 substrate peptide],
567 Sigma Aldrich / Merck Life Science, Oslo, Norway, Catalogue # 12-533). The N-terminus biotinylation of
568 the GSK3β substrate-peptide was performed using the "EZ-Link™ NHS-LC-Biotin" biotinylation kit from
569 Thermo Fisher Scientific (Thermo Fisher Scientific, Oslo, Norway, Catalogue # 21336) according to the
570 manufacturer's guidelines. Briefly, 50 ng of the biotinylated GSK3β substrate-peptide was immobilized in
571 each well of the Streptavidin-coated 96-well microplate. Experimental cell lysates (equivalent to 50 µg of
572 protein) were incubated with the immobilized biotinylated-GSK3β substrate overnight at 4°C, followed
573 by a 24-hour incubation with the specific detection-primary antibody (100 ng/well, 50 µL of 2 µg/mL)
574 directed against the phosphorylated-serine residue (***Supplementary Table S4***). The phosphorylated-
575 serine residue in the biotinylated-GSK3β substrate was then immunodetected using an AP (alkaline
576 phosphatase)-conjugated secondary antibody and the AP-substrate PNPP (p-Nitrophenyl Phosphate,
577 disodium salt) (Thermo Fisher Scientific, Oslo, Norway, Catalogue # 37621) as a chromophore for the
578 colorimetric read-out at 405 nm (λ405). GSK3β kinase activity assays were also conducted in the
579 presence of the GSK3β kinase inhibitor SB-216763 (Sigma Aldrich / Merck Millipore / Merck Life Science,
580 Darmstadt, Germany, Catalogue # S3442) to confirm assay specificity and serve as an experimental
581 blank. Optical density (O.D) values from the GSK3β kinase inhibitor-treated lysates were used for
582 experimental blank correction. Data is presented as experimental blank corrected O.D405 (λ405) values
583 from three technical replicates for each of the four biological replicates in each experimental group (n =
584 4).
585

586 ***Quantitative measurement of BAX and BAK in cytosolic and mitochondrial fractions using sandwich***
587 ***ELISA***

588 The levels of BAX and BAK in mitochondrial fractions, cytosolic fractions, and whole-cell lysates were
589 determined using a sandwich ELISA immunoassay. Briefly, 10-30 ng of the respective capture antibodies
590 (***Supplementary Table S4***) were immobilized in each well of 96-well microplates. Mitochondrial fractions
591 (equivalent to 20 µg of protein) and cytosolic fractions (equivalent to 40 µg of protein) were incubated
592 with the immobilized capture antibodies overnight at 4°C. After incubation, the conditioned
593 mitochondrial and cytosolic fractions were discarded, and the wells were washed three times (15
594 minutes each) with TBS-T. The wells were then incubated overnight at 4°C with the respective detection
595 antibodies (***Supplementary Table S4***). Following this, the wells were washed three times (15 minutes
596 each) with TBS-T and subjected to immunodetection using an HRP-conjugated secondary antibody and
597 the HRP-substrate OPD for colorimetric read-out at 450 nm (λ450). Antibody signal specificity was
598 confirmed through peptide blocking assays across all mitochondrial and cytosolic fractions from
599 experimental cells. The antibody blocking peptides corresponding to the specific epitopes for the
600 detection antibodies used are listed in ***Supplementary Table S4***. Absorbance values from the peptide
601 blocking assays were used for experimental blank correction. Data is presented as experimental blank
602 corrected O.D450 (λ450) values normalized to fold-change, derived from three technical replicates for
603 each of the four biological replicates in each experimental group (n = 4).
604

605 ***Isolation of heavy mitochondrial fractions for ELISA immunoassays***

606 Heavy mitochondrial fractions were isolated using the "Mitochondria Isolation Kit" from Sigma Aldrich /
607 Merck Millipore (Merck Life Science, Darmstadt, Germany, Catalogue # MITOISO2) as previously
608 described.[40] Briefly, AC-16 cells were terminally sub-cultured and plated in 150 mm cell-culture plates to

609 reach the desired confluence (2 x 10^7 cells per plate). After undergoing the specified transfection and
610 experimental procedures, the cells were trypsinized and pelleted by centrifugation at 600 x g for 5
611 minutes at 4°C. The cell pellets were resuspended in 1.2 mL of lysis buffer (provided with the kit)
612 containing protease inhibitors (also provided with the kit) and incubated on ice for 5 minutes to lyse the
613 cells. This was followed by the addition of twice the volume of extraction buffer (provided with the kit)
614 and centrifugation at 1000 x g for 10 minutes at 4°C. The resulting supernatant was further centrifuged
615 at 3500 x g for 10 minutes at 4°C to obtain the heavy mitochondrial fraction. For quantitative ELISA
616 immunoassays, the pelleted heavy mitochondrial fraction was resuspended in 200 µL of CelLytic™ M Cell
617 Lysis Reagent (provided with the kit) containing protease inhibitors (1:100 [v/v]).
618

619 ***Isolation and preparation of alkali-resistant outer mitochondrial membrane (OMM)-inserted and***
620 ***alkali-soluble OMM-tethered protein fractions for the quantitative measurement of OMM-inserted***
621 ***and OMM-tethered BAX and BAK***

622 To determine the abundance of oligomeric OMM-inserted BAX and BAK, the pelleted heavy
623 mitochondrial fraction (as described in Section M.9) was resuspended and incubated in 900 µL of 100
624 mM sodium carbonate (pH 11.5) at 4°C for 45 minutes, followed by ultracentrifugation at 144000 x g at
625 4°C for 45 minutes. The resulting pellet contained the alkali-resistant OMM-inserted protein fraction
626 with BAX and BAK oligomers, while the supernatant contained the alkali-soluble OMM-tethered protein
627 fraction with BAX and BAK monomers. The supernatants were neutralized with glacial acetic acid, and
628 the alkali-soluble proteins were precipitated using TCA (trichloroacetic acid), followed by centrifugation
629 at 15000 x g at 4°C for 60 minutes. The pellets from both the alkali-resistant OMM-inserted protein
630 fraction (containing BAX and BAK oligomers) and the alkali-soluble OMM-tethered protein fraction
631 (containing BAX and BAK monomers) were resuspended in denaturing RIPA lysis buffer (50 mM Tris, 150

632 mM NaCl, 0.5% w/v Sodium Deoxycholate, 0.1% w/v SDS, 1% v/v Triton-X, pH 7.4) supplemented with
633 protease and phosphatase inhibitors (Halt™ Protease and Phosphatase Inhibitor Cocktail 100x, Thermo
634 Fisher Scientific, Oslo, Norway, Catalogue # 78446). These fractions were then processed for ELISA
635 immunoassays to quantify the relative abundance of BAX and BAK and to validate the purity and
636 integrity of the fractions. Validation was performed by analyzing the presence and abundance of TOM40
637 (an OMM-inserted protein), TIM22 (an IMM-inserted protein), HK2 (an OMM-tethered protein), and
638 SDHA (an IMM-tethered protein).
639

640 ***DISC1 and GSK3β Co-Immunoprecipitation (Co-IP) Analysis***

641 Co-Immunoprecipitation (Co-IP) assays coupled with tandem ELISA immunoassays were performed to
642 determine the relative abundance of the DISC1 mutants in the GSK3β immunoprecipitates. AC-16 cells
643 (4×10^6) seeded in 100 mm plates, transfected and subjected to the experimental interventions (as
644 enunciated earlier), were homogenized using a *non-denaturing* lysis buffer (20 mM Tris, 137 mM Nacl, 2
645 mM EDTA, 1% Nonidet P-40, 10% glycerol, pH 7.4) supplemented with protease and phosphatase
646 inhibitors. The experimental cell lysates containing the equivalent to 750 µg of total protein was pre-
647 cleared by incubation with protein A/G coated agarose beads for 30 minutes at 4^0C to reduce the non-
648 specific binding of proteins to the beads. The equivalent of 750 µg of the pre-cleared lysate was
649 incubated separately, with either 5 µg of GSK3β antibody or 5 µg of the corresponding control rabbit IgG
650 antibody (***Supplementary Table S4***), overnight at 4^0C. The respective immunocomplexes were captured
651 and immobilized by the addition of protein A/G agarose beads and incubation overnight at 4^0C. The
652 beads containing the immunocomplexes were washed 3x with the *non-denaturing* lysis buffer followed
653 by centrifugation and discarder of the supernatant. The beads were suspended in *denaturing* RIPA
654 buffer (50 mM Tris, 150mM Nacl, 0.1% SDS, 0.5% sodium deoxycholate, 1% Triton X, pH 7.4)

655 supplemented with protease and phosphatase inhibitors and centrifuged to pellet the beads. The
656 supernatant containing the immunoprecipitated proteins was subjected to tandem ELISA with the
657 designated antibodies for DISC1 (***Supplementary Table S4***).
658

659 ***Integrity and validation of the fractionated mitochondrial and cytosolic compartments for Cytochrome***
660 ***C release assay and quantitative ELISA of BAX and BAK***

661 The integrity of the mitochondrial fraction was confirmed by the presence of COX4 and the absence of
662 β-Actin, while the cytosolic fraction's integrity was validated by the absence of COX4 and the presence
663 of β-Actin. Levels of COX4 and β-Actin in mitochondrial fractions, cytosolic fractions, and whole-cell
664 lysates were determined using a sandwich ELISA immunoassay. Briefly, 10-30 ng of the respective
665 capture antibodies (***Supplementary Table S4***) were immobilized in each well of 96-well microplates.
666 Mitochondrial fractions (20 µg of protein) and cytosolic fractions (40 µg of protein) were incubated with
667 the immobilized capture antibodies overnight at 4°C. After incubation, the conditioned fractions were
668 discarded, and the wells were washed three times (15 minutes each) with TBS-T. The wells were then
669 incubated overnight at 4°C with the respective detection antibodies (***Supplementary Table S4***).
670 Following this, the wells were washed three times (15 minutes each) with TBS-T and subjected to
671 immunodetection using an HRP-conjugated secondary antibody and the HRP-substrate Amplex Red (10-
672 acetyl-3,7-dihydroxyphenoxazine) (Thermo Fisher Scientific, Oslo, Norway, Catalogue # A22188) for
673 colorimetric read-out at 570 nm (λ570). Antibody signal specificity was confirmed through peptide
674 blocking assays across all mitochondrial and cytosolic fractions from experimental cells. The antibody
675 blocking peptides corresponding to the specific epitopes for the detection antibodies used are listed in
676 ***Supplementary Table S4***. Absorbance values from the peptide blocking assays were used for
677 experimental blank correction. Data is presented as experimental blank corrected O.D570 (λ570) values

678 normalized to fold-change, derived from three technical replicates for each of the four biological
679 replicates in each experimental group (n = 4).
680

681 ***Validation of the integrity of the alkali-resistant resistant outer mitochondrial membrane (OMM)-***
682 ***inserted and alkali soluble OMM-tethered protein fractions***

683 The integrity of the OMM-inserted protein fraction was validated by the presence of TOM40 and TIM22
684 concomitant with the absence of SDHA and HK2. The integrity of the OMM-tethered protein fraction
685 was validated by the absence of TOM40 and TIM22 concomitant with the presence of SDHA and HK2.
686 The levels of SDHA, HK2, TOM40, and TIM22, in the mitochondrial fractions, cytosolic fractions, as well
687 as the whole-cell lysates, were determined by *sandwich* ELISA immunoassay. Briefly, 10-30 ng of the
688 respective *capture* antibodies (***Supplementary Table S4***) were immobilized in each well of the respective
689 96-well microplates. The mitochondrial fractions (equivalent to 20 µg of protein content) and the
690 cytosolic fractions (equivalent to 40 µg of protein content) were incubated with the respective
691 immobilized *capture* antibodies, overnight at 4^0C. The conditioned mitochondrial fractions and cytosolic
692 fractions were discarded and the respective 96-well microplate wells were washed 3x (15 minutes each)
693 with TBS-T and incubated with the respective *detection* antibodies (***Supplementary Table S4***), overnight
694 at 4^0C. The 96-well microplate wells were washed 3x (15 min each) with TBS-T, followed by
695 immunodetection with the HRP-conjugated secondary antibody using the HRP-substrate TMB (3,3',5,5'-
696 tetramethylbenzidine) (Thermo Fisher Scientific, Oslo, Norway, Catalogue # N301) as a chromophore for
697 the colorimetric read-out (λ_{450}).The antibody signal specificity was established by performing peptide
698 blocking assays in the entire gamut of experimental samples. The antibody blocking peptides
699 corresponding to the specific epitopes for the respective *detection* antibodies used are enumerated in
700 ***Supplementary Table S4***. The respective absorbances from the peptide blocking assays were used for

701 the experimental blank correction. Data is expressed as experimental blank corrected $O.D_{450}$ (λ_{450}) values
702 normalized to *fold-change*, emanating from three technical replicates for each of the four biological
703 replicates belonging to each experimental group (n = 4).
704

705 ***Quantitative real-time RT-PCR analysis***

706 Total RNA was extracted from treated AC-16 cardiomyocytes using the "RNeasy Mini Kit" from Qiagen
707 (Qiagen Norge, Oslo, Norway, Catalogue # 74104) following the manufacturer's instructions and
708 protocols. cDNA was obtained by reverse transcribing 1 µg of extracted total RNA using the "QuantiTect
709 Reverse Transcription Kit" from Qiagen (Qiagen Norge, Oslo, Norway, Catalogue # 205313). cDNA
710 amplification was performed using the "miScript SYBR Green PCR Kit" from Qiagen (Qiagen Norge, Oslo,
711 Norway, Catalogue # 218075) following the manufacturer's instructions and protocols. The primer pair
712 used to amplify the *DISC1 mRNA transcript variant L* (NCBI Reference Sequence: NM_018662.3) was as
713 follows: *forward primer 5'- AGAGAGAGAAGGGCTGGAGG-3'* and *reverse primer 5'-*
714 *TGGAGCTGTAGGCTCTGGAT-3'.* The expression of specific amplified *DISC1* transcripts was normalized to
715 the expression of *actin beta (ACTB)* (NCBI Reference Sequence: NM_001101.5). The primer pair used to
716 amplify the *ACTB mRNA transcript* was as follows: *forward primer 5'- CTCGCCTTTGCCGATCC-3'* and
717 *reverse primer 5'- TCTCCATGTCGTCCCAGTTG-3'.* The expression of specific amplified *DISC1* transcripts
718 was normalized to the expression of *ACTB* using the *delta delta* C_T method.[51]
719 <u>*Cardiac samples from CABG left ventricle myocardium*</u> biopsies were stored at -80 °C in RNAlater. After
720 thawing, the biopsies were washed with RNase-free water and excess water remover by bloting againg
721 paper and transferring to new tubes with 4 ceramic beads and 300 µl of RTL lysis buffer. RNA extraction
722 was performed using an RNeasy kit for fibrous tissues (Qiazol) according the manufacturer's protocol.
723 cDNA was obtained using a Quantitech reverse transcription kit (Qiagen) according to the

724 manufacturer's protocol. Quantification was performed by DISC1 Primer Assays from Qiagen (Qiagen
725 QuantiTect Primer Assay (QT01019060) normalized to B2M as a housekeeping gene. For detection of
726 DISC1 RNA expression in *blood from CABG patients*, RNA was isolated from PAXgene tubes
727 (PreAnalytiX,Qiagen, Hilden, Germany), using NAxtra™ Blood total nucleic acid extraction kit (Lybe
728 Scientific, Trondheim, Norway) according to manufacturer's protocol.[52] Briefly, blood was spun down
729 and supernatant removed, and protein digested using Proteinase K. Using a Kingfisher Flex
730 (ThermoFisher), samples were then incubated in a lysis buffer, nucleic acid bound to magnetic beads,
731 DNA was digested, and samples were washed. RNA was quantified using a Qubit RNA HS Assay Kit
732 (Invitrogen). cDNA was reverse transcribed from these samples using QuantiTect Reverse Transcription
733 Kit (Qiagen) according to manufacturer's protocol. DISC1 mRNA was quantified by RT-PCR, using
734 QuantiTect SYBR Green PCR Kit (Qiagen) according to the manufacturer's protocol. Reactions were run
735 in a CFX Opus Real Time PCR system (Bio-Rad). The primer pair used to amplify the DISC1 mRNA
736 transcript variant L was the same as described above for human AC16 cardiomyocytes. The expression
737 of specific amplified *DISC1* transcripts was normalized to the expression of Homo sapiens hypoxanthine
738 phosphoribosyltransferase (HPRT) (NCBI Reference Sequence: NM_000194). The primer pair used to
739 amplify the HPRT mRNA transcript was as follows: *forward primer 5'- CCTGGCGTCGTGATTAGTGAT -3'*
740 and *reverse primer 5'-* AGACGTTCAGTCCTGTCCATAA *-3'* (Source: Primerbank 164518913c1[53]). The
741 expression of specific amplified *DISC1* transcripts was normalized to the expression of HPRT using the
742 *delta delta* C_T method.[51]
743 *For rat tissue*, cDNA was obtained using the QuantiTect Reverse Transcription Kit (Qiagen) following the
744 manufacturer's instructions. qRT-PCRs were performed using a QuantiTect SYBR Green PCR Kit (Qiagen).
745 The primer pair used to amplify DISC1 in rats was as follows: *forward primer 5'-*
746 *GACAGTGGTTGTCGGCAAGAAT-3'* and *reverse primer 5'-TGCTCCAAGCTACATCAAGGC-3'.* PCR

747 amplification was performed using "*CFX96 Real-Time PCR Detection*" from Bio-Rad (Bio-Rad Norway AS,
748 Oslo, Norway) in all samples.
749

750 ***Declaration of generative AI and AI-assisted technologies in the writing process***

751 During the preparation of this work the authors used [Microsoft Copilot] in order to lighty improve
752 language and readability. After using this tool, the authors reviewed and edited the content as needed
753 and take full responsibility for the content of the publication.
754

755 ***Statistical analyses***

756 Statistical analysis was performed with GraphPad Prism 10 (GraphPad Software, San Diego, CA, USA).
757 Quantitative data for all the assays are presented as Mean values ± s.e.m. (Standard Error of the mean).
758 Relevant statistical methods are presented in each data set.
759
760

761 ***Acknowledgment***

762 The current project was financed by grants from the Research Council Norway – FRIPRO ID 316002 to
763 MAH. The project was also funded by Foundation Dam (grant number: FOR555614) to MAH. This study
764 is further supported by The National Institute of Mental Health Grants MH-094268, MH-105660, and
765 MH129480 to AS. The RNA library prep, sequencing and bioinformatics analysis were performed in close
766 collaboration with the Genomics Core Facility (GCF), Norwegian University of Science and Technology
767 (NTNU). We especially acknowledge Arnar Flatberg for bioinformatics analyses. GCF is funded by the

768 Faculty of Medicine and Health Sciences at NTNU and Central Norway Regional Health Authority. We
769 acknowledge Dr. Karin Garten for contribution to the method of determining infarct size in TTC stained
770 cardiac tissue.
771

772 ***Author contributions***

773 Conceptualization: MAH
774 Methodology: GM, MP, NRS, RER, FJE, KY, KI, CAAC, KP, RKN, MAH
775 Investigation: GM, MP, KH, AW, NRS, RB, RER, RKN, FJE, KY, KI, CAAC, KP, GB, AS, MAH
776 Visualization: MAH, GM, KP, NRS
777 Supervision: MAH, AS
778 Writing—original draft: MAH
779 Writing—review & editing: GM, MP, KH, AW, NRS, RB, RER, FJE, KY, KI, CAAC, RKN, KP, GB, AS, MAH
780
781
782

783 # References

784

785 1. Organization WH. Global status report on noncommunicable diseases 2014. *WHOint*.
786 2014.
787 2. Hausenloy DJ, Garcia-Dorado D, Botker HE, Davidson SM, Downey J, Engel FB, Jennings
788 R, Lecour S, Leor J, Madonna R, et al. Novel targets and future strategies for acute
789 cardioprotection: Position Paper of the European Society of Cardiology Working Group
790 on Cellular Biology of the Heart. *Cardiovasc Res*. 2017;113:564-585. doi:
791 10.1093/cvr/cvx049
792 3. Creemers EE, Wilde AA, Pinto YM. Heart failure: advances through genomics. *Nature*
793 *reviews Genetics*. 2011;12:357-362. doi: 10.1038/nrg2983

4. Lecour S, Botker HE, Condorelli G, Davidson SM, Garcia-Dorado D, Engel FB, Ferdinandy P, Heusch G, Madonna R, Ovize M, et al. ESC working group cellular biology of the heart: position paper: improving the preclinical assessment of novel cardioprotective therapies. *Cardiovasc Res*. 2014;104:399-411. doi: 10.1093/cvr/cvu225
5. Ibanez B, Heusch G, Ovize M, Van de Werf F. Evolving therapies for myocardial ischemia/reperfusion injury. *J Am Coll Cardiol*. 2015;65:1454-1471. doi: 10.1016/j.jacc.2015.02.032
6. Parviz Y, Waleed M, Vijayan S, Adlam D, Lavi S, Al Nooryani A, Iqbal J, Stone GW. Cellular and molecular approaches to enhance myocardial recovery after myocardial infarction. *Cardiovasc Revasc Med*. 2019;20:351-364. doi: 10.1016/j.carrev.2018.05.021
7. Brandon NJ, Sawa A. Linking neurodevelopmental and synaptic theories of mental illness through DISC1. *Nat Rev Neurosci*. 2011;12:707-722. doi: 10.1038/nrn3120
8. Niwa M, Cash-Padgett T, Kubo KI, Saito A, Ishii K, Sumitomo A, Taniguchi Y, Ishizuka K, Jaaro-Peled H, Tomoda T, et al. DISC1 a key molecular lead in psychiatry and neurodevelopment: No-More Disrupted-in-Schizophrenia 1. *Mol Psychiatry*. 2016;21:1488-1489. doi: 10.1038/mp.2016.154
9. Blackwood DH, Fordyce A, Walker MT, St Clair DM, Porteous DJ, Muir WJ. Schizophrenia and affective disorders--cosegregation with a translocation at chromosome 1q42 that directly disrupts brain-expressed genes: clinical and P300 findings in a family. *Am J Hum Genet*. 2001;69:428-433. doi: 10.1086/321969
10. Doyle OM, Bois C, Thomson P, Romaniuk L, Whitcher B, Williams SC, Turkheimer FE, Stefansson H, McIntosh AM, Mehta MA, et al. The cortical thickness phenotype of individuals with DISC1 translocation resembles schizophrenia. *J Clin Invest*. 2015;125:3714-3722. doi: 10.1172/JCI82636
11. St Clair D, Blackwood D, Muir W, Carothers A, Walker M, Spowart G, Gosden C, Evans HJ. Association within a family of a balanced autosomal translocation with major mental illness. *Lancet*. 1990;336:13-16. doi: 10.1016/0140-6736(90)91520-k
12. Porteous DJ, Millar JK, Brandon NJ, Sawa A. DISC1 at 10: connecting psychiatric genetics and neuroscience. *Trends Mol Med*. 2011;17:699-706. doi: 10.1016/j.molmed.2011.09.002
13. Laursen TM, Munk-Olsen T, Vestergaard M. Life expectancy and cardiovascular mortality in persons with schizophrenia. *Curr Opin Psychiatry*. 2012;25:83-88. doi: 10.1097/YCO.0b013e32835035ca
14. Laursen TM, Wahlbeck K, Hällgren J, Westman J, Ösby U, Alinaghizadeh H, Gissler M, Nordentoft M. Life expectancy and death by diseases of the circulatory system in patients with bipolar disorder or schizophrenia in the Nordic countries. *PLoS One*. 2013;8:e67133. doi: 10.1371/journal.pone.0067133
15. Gale CR, Batty GD, Osborn DP, Tynelius P, Rasmussen F. Mental disorders across the adult life course and future coronary heart disease: evidence for general susceptibility. *Circulation*. 2014;129:186-193. doi: 10.1161/circulationaha.113.002065
16. Goff DC, Sullivan LM, McEvoy JP, Meyer JM, Nasrallah HA, Daumit GL, Lamberti S, D'Agostino RB, Stroup TS, Davis S, et al. A comparison of ten-year cardiac risk estimates in schizophrenia patients from the CATIE study and matched controls. *Schizophr Res*. 2005;80:45-53. doi: 10.1016/j.schres.2005.08.010

838 17. Crump C, Winkleby MA, Sundquist K, Sundquist J. Comorbidities and Mortality in
839 Persons With Schizophrenia: A Swedish National Cohort Study. *American Journal of*
840 *Psychiatry*. 2013;170:324-333. doi: 10.1176/appi.ajp.2012.12050599
841 18. Korkmaz S, Korkmaz H, Ozer O, Atmaca M. Assessment of left ventricle systolic and
842 diastolic functions in schizophrenia patients. *Psychiatry Res*. 2016;240:348-351. doi:
843 10.1016/j.psychres.2016.04.025
844 19. Pillinger T, Osimo EF, de Marvao A, Berry MA, Whitehurst T, Statton B, Quinlan M,
845 Brugger S, Vazir A, Cook SA, et al. Cardiac structure and function in patients with
846 schizophrenia taking antipsychotic drugs: an MRI study. *Transl Psychiatry*. 2019;9:163.
847 doi: 10.1038/s41398-019-0502-x
848 20. Liu JM, Liu A, Leal J, McMillan F, Francis J, Greiser A, Rider OJ, Myerson S, Neubauer S,
849 Ferreira VM, et al. Measurement of myocardial native T1 in cardiovascular diseases and
850 norm in 1291 subjects. *J Cardiovasc Magn Reson*. 2017;19:74. doi: 10.1186/s12968-017-
851 0386-y
852 21. John JP, Thirunavukkarasu P, Ishizuka K, Parekh P, Sawa A. An in-silico approach for
853 discovery of microRNA-TF regulation of DISC1 interactome mediating neuronal
854 migration. *NPJ Syst Biol Appl*. 2019;5:17. doi: 10.1038/s41540-019-0094-3
855 22. Barodia SK, Park SK, Ishizuka K, Sawa A, Kamiya A. Half-life of DISC1 protein and its
856 pathological significance under hypoxia stress. *Neurosci Res*. 2015;97:1-6. doi:
857 10.1016/j.neures.2015.02.008
858 23. Ferguson TB, Jr. Ischemia/reperfusion injury in coronary artery bypass grafting: time to
859 revisit? *J Thorac Cardiovasc Surg*. 2011;141:1-2. doi: 10.1016/j.jtcvs.2010.04.008
860 24. Hausenloy DJ, Candilio L, Laing C, Kunst G, Pepper J, Kolvekar S, Evans R, Robertson S,
861 Knight R, Ariti C, et al. Effect of remote ischemic preconditioning on clinical outcomes in
862 patients undergoing coronary artery bypass graft surgery (ERICCA): rationale and study
863 design of a multi-centre randomized double-blinded controlled clinical trial. *Clin Res*
864 *Cardiol*. 2012;101:339-348. doi: 10.1007/s00392-011-0397-x
865 25. Brener SJ, Lytle BW, Schneider JP, Ellis SG, Topol EJ. Association between CK-MB
866 elevation after percutaneous or surgical revascularization and three-year mortality. *J Am*
867 *Coll Cardiol*. 2002;40:1961-1967. doi: 10.1016/s0735-1097(02)02538-x
868 26. Ruiz-Meana M, Abellan A, Miro-Casas E, Agullo E, Garcia-Dorado D. Role of sarcoplasmic
869 reticulum in mitochondrial permeability transition and cardiomyocyte death during
870 reperfusion. *Am J Physiol Heart Circ Physiol*. 2009;297:H1281-1289. doi:
871 10.1152/ajpheart.00435.2009
872 27. Griffiths EJ, Halestrap AP. Mitochondrial non-specific pores remain closed during cardiac
873 ischaemia, but open upon reperfusion. *Biochem J*. 1995;307 (Pt 1):93-98.
874 28. Ertracht O, Malka A, Atar S, Binah O. The mitochondria as a target for cardioprotection
875 in acute myocardial ischemia. *Pharmacol Ther*. 2014;142:33-40. doi:
876 10.1016/j.pharmthera.2013.11.003
877 29. Halestrap AP, Clarke SJ, Khaliulin I. The role of mitochondria in protection of the heart
878 by preconditioning. *Biochim Biophys Acta*. 2007;1767:1007-1031. doi:
879 10.1016/j.bbabio.2007.05.008

880 30. Hausenloy DJ, Yellon DM. The mitochondrial permeability transition pore: its
881 fundamental role in mediating cell death during ischaemia and reperfusion. *J Mol Cell*
882 *Cardiol*. 2003;35:339-341.
883 31. Ohori K, Miura T, Tanno M, Miki T, Sato T, Ishikawa S, Horio Y, Shimamoto K. Ser9
884 phosphorylation of mitochondrial GSK-3beta is a primary mechanism of cardiomyocyte
885 protection by erythropoietin against oxidant-induced apoptosis. *Am J Physiol Heart Circ*
886 *Physiol*. 2008;295:H2079-2086. doi: 10.1152/ajpheart.00092.2008
887 32. Saundh SL, Patnaik D, Gagne S, Bishop JA, Lipsit S, Amat S, Pujari N, Nambisan AK, Bigsby
888 R, Murphy M, et al. Identification and Mechanistic Characterization of a Peptide
889 Inhibitor of Glycogen Synthase Kinase (GSK3beta) Derived from the Disrupted in
890 Schizophrenia 1 (DISC1) Protein. *ACS Chem Neurosci*. 2020;11:4128-4138. doi:
891 10.1021/acschemneuro.0c00380
892 33. Ibanez B, James S, Agewall S, Antunes MJ, Bucciarelli-Ducci C, Bueno H, Caforio ALP,
893 Crea F, Goudevenos JA, Halvorsen S, et al. 2017 ESC Guidelines for the management of
894 acute myocardial infarction in patients presenting with ST-segment elevation: The Task
895 Force for the management of acute myocardial infarction in patients presenting with ST-
896 segment elevation of the European Society of Cardiology (ESC). *Eur Heart J*.
897 2018;39:119-177. doi: 10.1093/eurheartj/ehx393
898 34. Juhaszova M, Zorov DB, Kim SH, Pepe S, Fu Q, Fishbein KW, Ziman BD, Wang S, Ytrehus
899 K, Antos CL, et al. Glycogen synthase kinase-3beta mediates convergence of protection
900 signaling to inhibit the mitochondrial permeability transition pore. *J Clin Invest*.
901 2004;113:1535-1549. doi: 10.1172/jci19906
902 35. Zhu M, Feng J, Lucchinetti E, Fischer G, Xu L, Pedrazzini T, Schaub MC, Zaugg M. Ischemic
903 postconditioning protects remodeled myocardium via the PI3K-PKB/Akt reperfusion
904 injury salvage kinase pathway. *Cardiovasc Res*. 2006;72:152-162. doi:
905 10.1016/j.cardiores.2006.06.027
906 36. Gomez L, Paillard M, Thibault H, Derumeaux G, Ovize M. Inhibition of GSK3beta by
907 postconditioning is required to prevent opening of the mitochondrial permeability
908 transition pore during reperfusion. *Circulation*. 2008;117:2761-2768. doi:
909 10.1161/circulationaha.107.755066
910 37. Juhaszova M, Zorov DB, Yaniv Y, Nuss HB, Wang S, Sollott SJ. Role of glycogen synthase
911 kinase-3beta in cardioprotection. *Circ Res*. 2009;104:1240-1252. doi:
912 10.1161/circresaha.109.197996
913 38. Yang K, Chen Z, Gao J, Shi W, Li L, Jiang S, Hu H, Liu Z, Xu D, Wu L. The Key Roles of GSK-
914 3β in Regulating Mitochondrial Activity. *Cell Physiol Biochem*. 2017;44:1445-1459. doi:
915 10.1159/000485580
916 39. Zhang M, Zheng J, Nussinov R, Ma B. Release of Cytochrome C from Bax Pores at the
917 Mitochondrial Membrane. *Sci Rep*. 2017;7:2635. doi: 10.1038/s41598-017-02825-7
918 40. Marwarha G, Rosand O, Slagsvold KH, Hoydal MA. GSK3beta Inhibition Is the Molecular
919 Pivot That Underlies the Mir-210-Induced Attenuation of Intrinsic Apoptosis Cascade
920 during Hypoxia. *Int J Mol Sci*. 2022;23. doi: 10.3390/ijms23169375
921 41. Green DR. Apoptotic Pathways: Paper Wraps Stone Blunts Scissors. *Cell*. 2000;102:1-4.
922 doi: https://doi.org/10.1016/S0092-8674(00)00003-9

42. Salvesen GS. Caspases: opening the boxes and interpreting the arrows. *Cell Death & Differentiation*. 2002;9:3-5. doi: 10.1038/sj.cdd.4400963
43. Earnshaw WC, Martins LM, Kaufmann SH. Mammalian caspases: structure, activation, substrates, and functions during apoptosis. *Annu Rev Biochem*. 1999;68:383-424. doi: 10.1146/annurev.biochem.68.1.383
44. Nicholson DW, Ali A, Thornberry NA, Vaillancourt JP, Ding CK, Gallant M, Gareau Y, Griffin PR, Labelle M, Lazebnik YA, et al. Identification and inhibition of the ICE/CED-3 protease necessary for mammalian apoptosis. *Nature*. 1995;376:37-43. doi: 10.1038/376037a0
45. Honda HM, Korge P, Weiss JN. Mitochondria and ischemia/reperfusion injury. *Ann N Y Acad Sci*. 2005;1047:248-258. doi: 10.1196/annals.1341.022
46. Dweep H, Gretz N. miRWalk2.0: a comprehensive atlas of microRNA-target interactions. *Nat Methods*. 2015;12:697. doi: 10.1038/nmeth.3485
47. von Mering C, Jensen LJ, Snel B, Hooper SD, Krupp M, Foglierini M, Jouffre N, Huynen MA, Bork P. STRING: known and predicted protein-protein associations, integrated and transferred across organisms. *Nucleic Acids Res*. 2005;33:D433-437. doi: 10.1093/nar/gki005
48. Kemi OJ, Hoydal MA, Haram PM, Garnier A, Fortin D, Ventura-Clapier R, Ellingsen O. Exercise training restores aerobic capacity and energy transfer systems in heart failure treated with losartan. *Cardiovasc Res*. 2007;76:91-99. doi: 10.1016/j.cardiores.2007.06.008
49. Freshney RI. *Culture of Animal Cells: A Manual of Basic Technique and Specialized Applications, Sixth Edition*. Wiley-Blackwell; 2010.
50. Freshney RI. *Culture of Animal Cells: A Manual of Basic Technique and Specialized Applications, 7th Edition*. Wiley-Blackwell; 2016.
51. Silva FBE, Vaisman M, Ponce T, de Barros TR, CB ES, Salerno VP, Mainenti MRM. A systematic review of hormone levels, biomarkers of cellular injury and oxidative stress in multi-stressor military field training exercises. *Arch Endocrinol Metab*. 2022;66:382-389. doi: 10.20945/2359-3997000000443
52. Starheim EJ, Ravlo E, Schjolberg JO, Solvang V, Wang W, Scrimgeour NR, Manaf A, Erlandsen SE, Aas PA, Hagen L, et al. NAxtra magnetic nanoparticles for low-cost, efficient isolation of mammalian DNA and RNA. *Sci Rep*. 2023;13:20836. doi: 10.1038/s41598-023-46868-5
53. Wang X, Spandidos A, Wang H, Seed B. PrimerBank: a PCR primer database for quantitative gene expression analysis, 2012 update. *Nucleic Acids Res*. 2012;40:D1144-1149. doi: 10.1093/nar/gkr1013

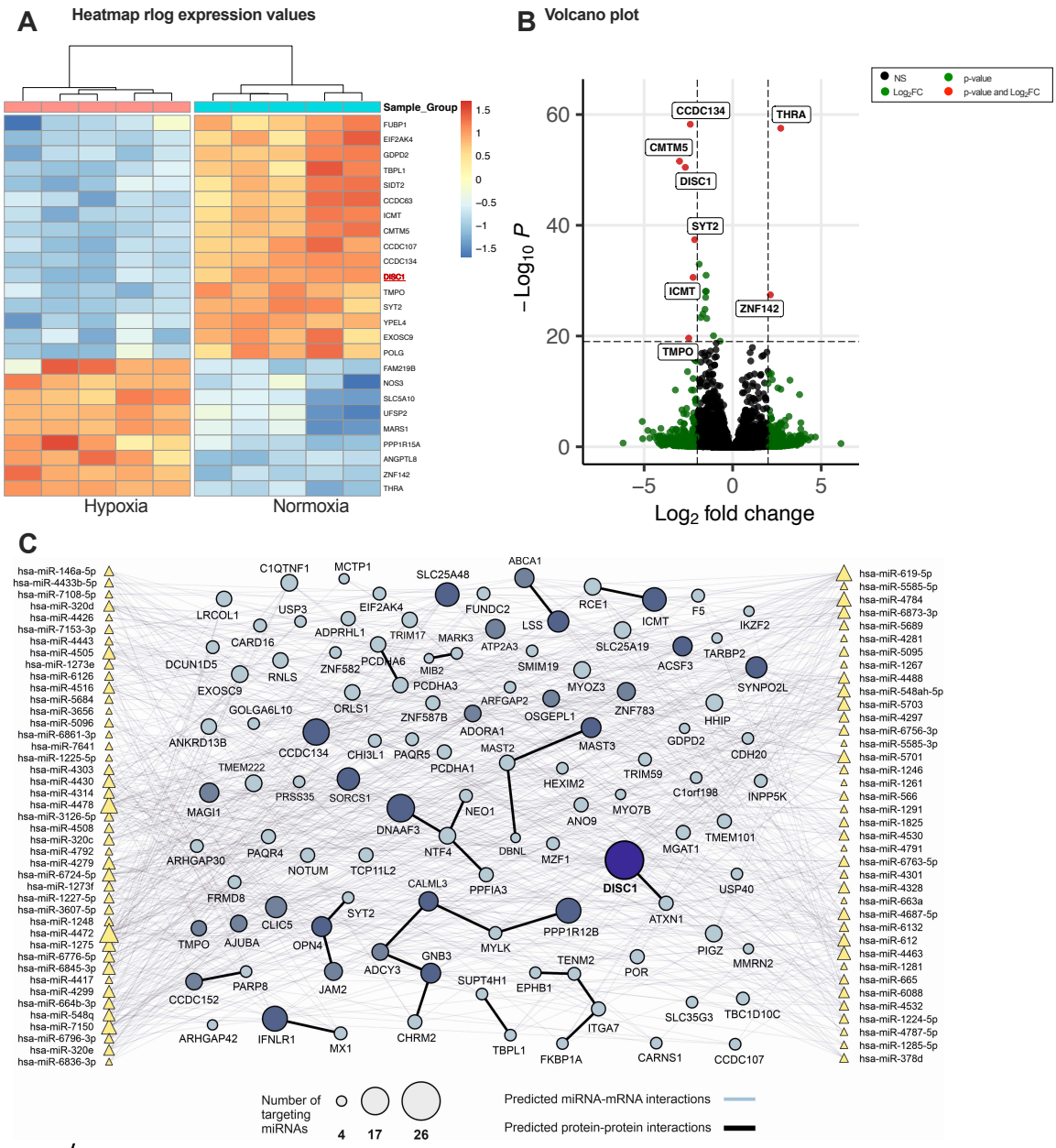

961
962 ***Fig. 1 /Discovering DISC1 by transcriptomics***

963 **A,** Heatmap of RNA sequencing data of the coding RNA with a cutoff value of $10E^{-10}$ and a Log_2FC cutoff
964 >2. **B**, Volcano plot displaying all regulated coding mRNA transcripts including statistical analyses with
965 cut-off $-Log_{10}$ P value < $10E^{-20}$ and $-Log_2$ fold change value ± 2, mitochondrial mRNA are left out for
966 simplicity in A-B (all data included in online supplements). **C**, Regulatory networks in hypoxia-stimulated
967 hIPSC-cardiomyocytes relationships between upregulated microRNAs (miRs) and their downregulated
968 mRNA targets. Upregulated miRNAs are depicted as triangles, whose sizes are related to the number of
969 targets; mRNAs are represented by circles; black lines represent the interaction between proteins
970 encoded by each gene extracted from STRING (combined score >0.8) (Supporting data in Excel file, E3).

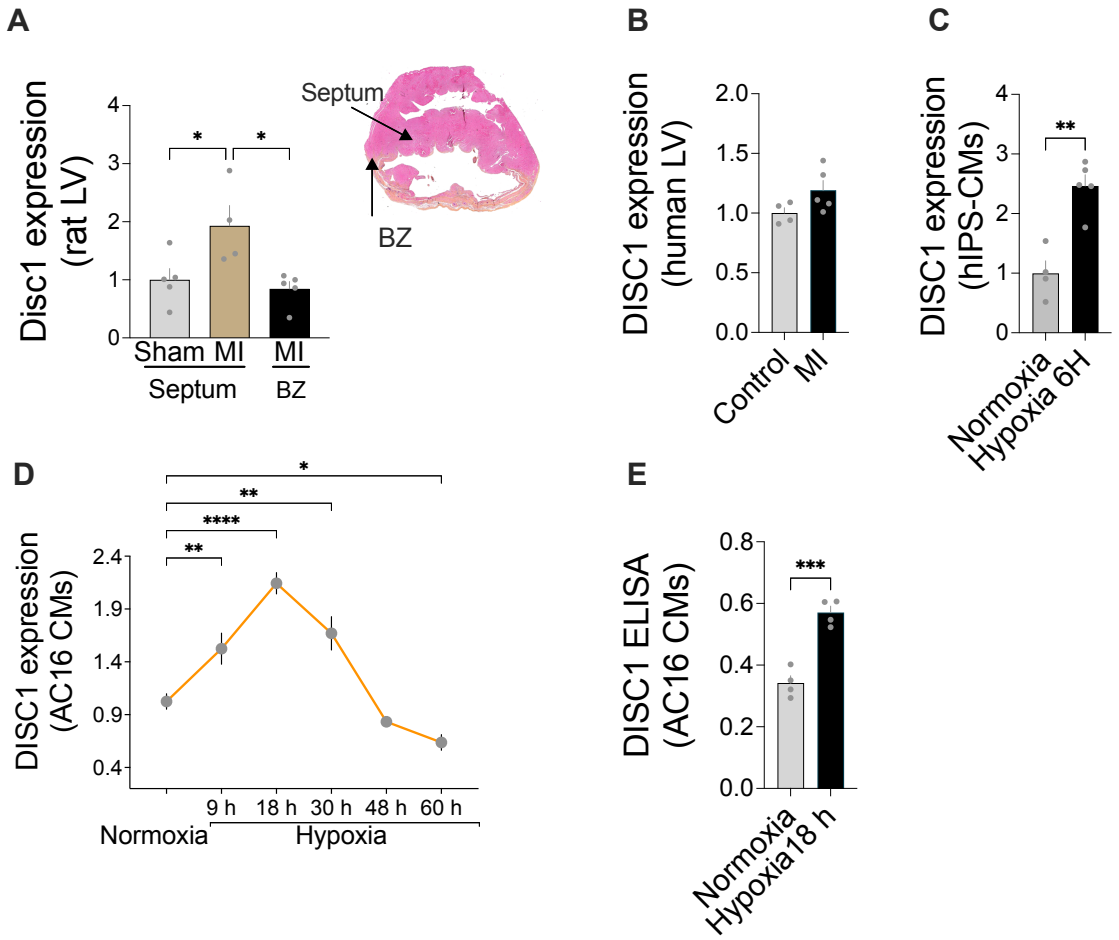

Fig. 2 /Expressional regulation of DISC1 in myocardial infarction and cardiomyocyte hypoxia

A, DISC1 mRNA expression changes in post-myocardial infarction (MI) rat hearts from sham-operated animals and regional areas distant from the MI (sham, N=5; MI septum, N=4: MI border zone (BZ), N=5). Zones of harvesting displayed by exemplary rat heart with MI. **B**, DISC1 mRNA expression in CABG patient biopsies from the non-infarcted area of the left ventricle of post-MI heart failure patients (N=5) vs. non-MI controls (N=4). **C**, Quantification of DISC1 mRNA transcripts in hiPS-CM following 6 hours of hypoxia (1% O_2). **D**, Timeline of DISC1 mRNA expression in human AC16 CMs following normoxia and hypoxia. **E**, DISC1 total protein expression following 18 hours of hypoxia in AC16 CMs. Data presented as fold change(A-D); E is expressed as absorbances measured at λ_{450} (450 nm), data presented as mean ± s.e.m. P values are indicated by : ** P<0.05, ** P<0.01, *** P<0.001, **** P<0.0001*. Statistical analyses in A performed by one-way ANOVA and Tukey's post hoc test; B, C and E performed by unpaired t-test; D, performed by one-way ANOVA compared to normoxia. All analyses performed using two-tailed analyses.

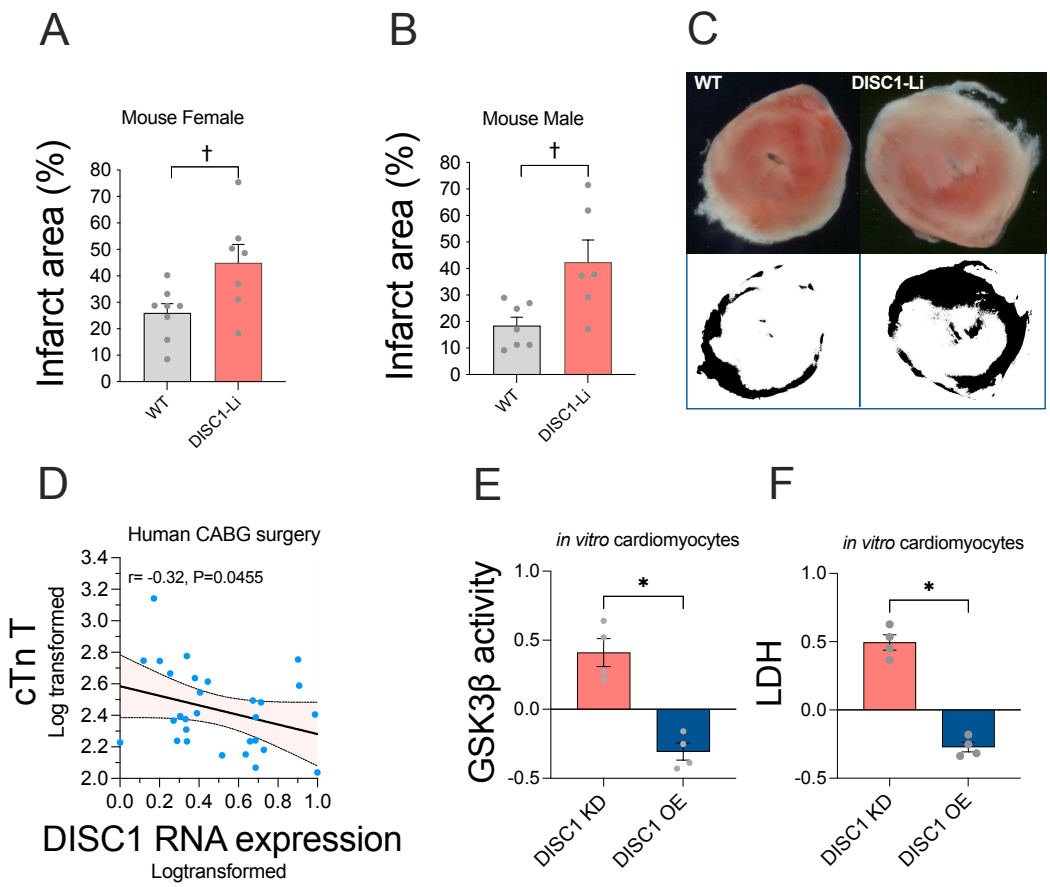

Fig. 3 / Reduced DISC1 expression increases cardiac damage following ischemic and hypoxic stress, in mouse models, Coronary Artery Bypass Grafting (CABG) patients and in vitro cardiomyocyte models

A-B, Myocardial infarct size in WT and DISC1-Li mice after 30 minutes of global ischemia followed by 1 h 40 m of reperfusion in male mice (WT, n=7/DISC1-Li, n=6) and female mice (WT, n=7/DISC1-Li, n=7). **C**, Exemplary images from WT and DISC-Li Male. The black/white image shows the infarct area in black. **D**, Data from CABG patients showing the delta release of cardiac Troponin T (cTnT) from preoperative to 24 hours postoperative, compared to DISC1 RNA expression in blood measured preoperatively (N=29). Figures **E-F** represent experiments in in AC16 cardiomyocytes to determine the effect of both DISC1 silencing using short hairpin (sh)RNA pLKO.1-DISC1 (**DISC1 KD**) compared to respective pLKO.1- empty vector or by overexpression of DISC1 using pRK5-DISC1 overexpression vector (DISC1 OE) compared to respective pRK5-EV. All data are presented in relation to the fractional difference from respective Mock (zero line). **E**, GSK3β activity and **F**, Lactate dehydrogenase released from cardiomyocytes to cytosol. Statistical analyzes in A-B are performed using two-tailed t-test († *P<0.05,* difference between WT and DISC1-Li mice). Data in panel D exhibited a lognormal distribution and were log-transformed for both cardiac Troponin T (cTnT) and DISC1 RNA expression. Correlation was analysed using one-tailed Pearson correlation. Statistical analyses in E-F were performed using using two-tailed t-test to assess the difference in response compared to respective Mock between DISC1 KD versus DISC1 OE. Statistical difference displayed by: ** P<0.05, ** P<0.01, *** P<0.001.*

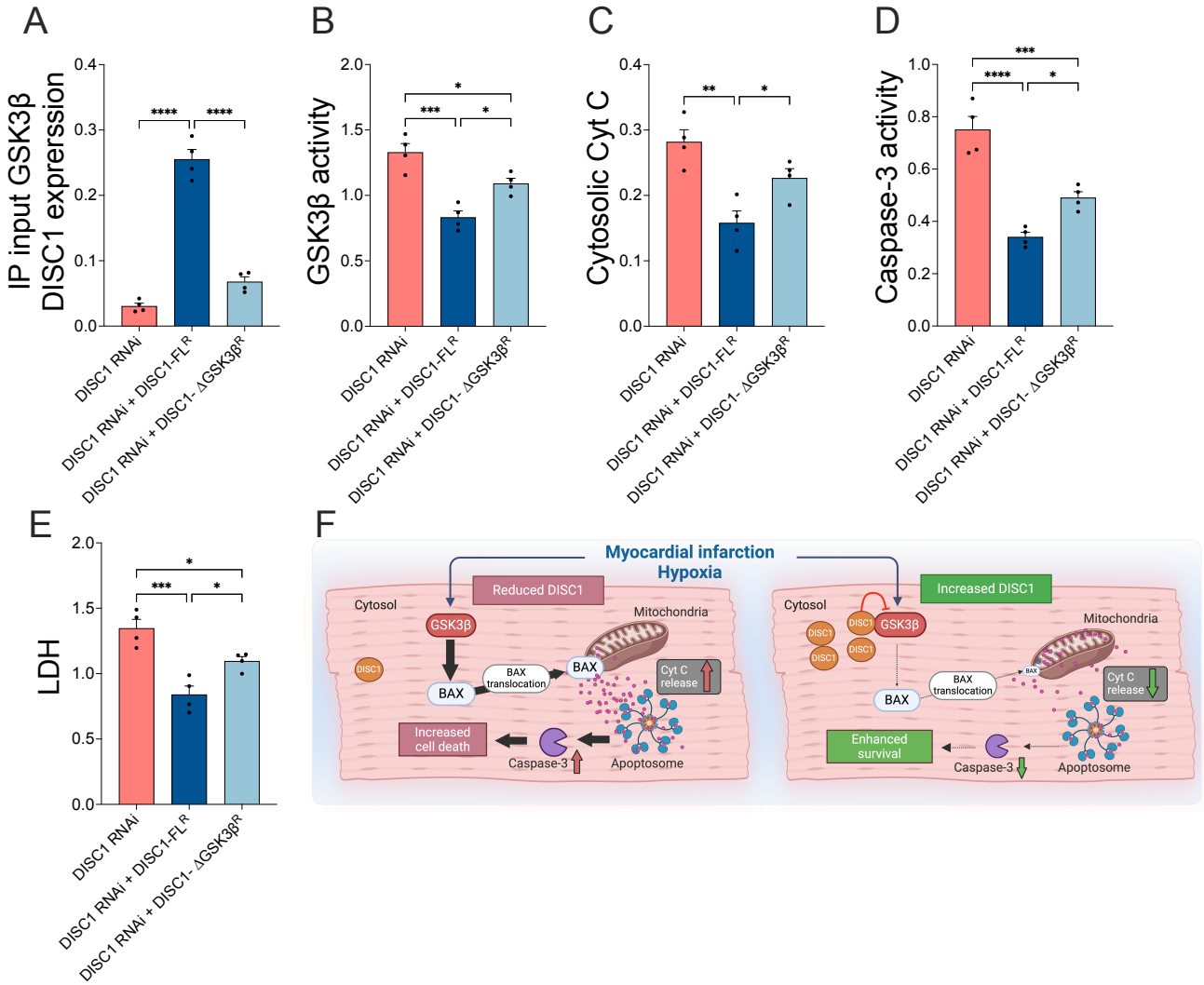

Fig. 4 / Direct DISC1- GSK3β interaction hinder GSK3β activation and reduces cytosolic Cytochrome C (Cyt C) release and caspase-3 activity

To further asses the role of DISC1 on GSK3β activity during hypoxia, the experiments were performed using the following scenarios; 1) **DISC1 RNAi**, expression of the not resistant to shRNA full length (FL) (DISC1-FL) + co-treatment by shRNA to silence the DISC1, leaving cells with low DISC1 expression as product; 2) **DISC1 RNAi + DISC1-FL^R**: overexpression of DISC1-FL^R that is resistant to shRNA and 3) **DISC1 RNAi + DISC1- ΔGSK3β^R**, which is the DISC1 overexpression vector with triple mutation at the binding site of GSK3β and resistant to DISC1 RNAi. All experimental groups received treatment with shRNA DISC1 to remove contribution from the endogenous DISC1, thus leaving mainly the product from the respective overexpression vectors, ^{R} denotes resistant to this shRNA (i.e. DISC1-FL^R and DISC1- ΔGSK3β^R). **A**, DISC1-

1017 GSK3β interaction by IP; **B**, GSK3β activity; **C**, cytosolic Cyt C levels; **D**, Caspase-3 activity; **E**, Lactate
1018 dehydrogenase (LDH) from cardiomyocytes released to medium. **F**, Simplified overview displaying the
1019 effect of low DISC1 levels with consequences of interrupted DISC1- GSK3β interaction causing increased
1020 cell death, whereas increased DISC1 levels causes maintained DISC1- GSK3β interaction with
1021 consequences of reduced GSK3β activity and enhanced survival. All data are presented as mean ± s.e.m.
1022 Statistical analyses were performed by one-way ANOVA with Tukey's post hoc correction for multiple
1023 comparisons. ** P<0.05; **P<0.01; ***P<0.001; ****P<0.0001*.
1024
1025
1026